Research Report – UCD-ITS-RR-12-12

A First-Order Transient Response Model for Lithium-ion Batteries of Various Chemistries: Test Data and Model Validation

September 2012

Siqi Lin
Hengbing Zhao
Andrew Burke

Institute of Transportation Studies ◦ University of California, Davis
One Shields Avenue ◦ Davis, California 95616
PHONE (530) 752-6548 ◦ FAX (530) 752-6572
www.its.ucdavis.edu

A First-Order Transient Response Model for Lithium-ion Batteries of Various Chemistries: Test Data and Model Validation

UCD-ITS-RR-12-12

September 2012

By

Siqi Lin

(Beijing Jiaotong University, China)

Hengbing Zhao

Andrew Burke

Institute of Transportation Studies

University of California-Davis

Abstract

In this report, a first-order transient response battery model is presented. The model can be utilized in the simulation of electric vehicles to calculate the battery voltage for dynamic operation of an electric-hybrid vehicle on various driving cycles. The battery model requires knowledge of the battery Ah capacity, the hyst-SOC-OCV curve and parameters of the equivalent circuit (R_0, R_1, tau1). A number of lithium-ion cells of the different chemistries were tested on charge / discharge step current profiles to determine the circuit parameters for a series of states-of-charge. The cells were then tested on the MHC and DST variable current profiles to determine how well the model predicted the response of the cells to the dynamic profiles. For DST test, the output voltages from the model for all the eight cells tested followed the test voltages well with the errors being relatively small –usually less than 20mV – except for SOC near to 1 and O. For MHC profile, the tests were performed at a nearly fixed SOC and the errors were particularly small. The study shows that over most of the useable state-of-charge range, the first-order transient model can be applied to predict the voltage response of lithium-ion batteries to dynamic charge and discharge currents encountered in vehicle applications.

A First-Order Transient Response Model for Lithium-ion Batteries of Various Chemistries: Test data and model validation

Abstract

1. Introduction

2. First-Order Transient Response Model

3. Test Procedures

- 3.1 Tested Cells and Test Conditions
- 3.2 Ah Capacity Test
- 3.3 Hyst-SOC-OCV Curve test
  - a. SOC Definition
  - b. Hyst-SOC-OCV curve
- 3.4 Circuit elements test
- 3.5 Hybrid Pulse Power Characterization (HPPC) Test
- 3.6 MHC Test
- 3.7 Dynamic Stress Test

4. Test Results and Model Validation

- 4.1 Altairnano 50Ah Cell
  - a. Hyst-SOC-OCV curve
  - b. parameter R0, R1 and Tau1
  - c. MHC test
  - d. DST test
  - e. General comments
- 4.2 EIG 20Ah NiCo cell
  - a. Hyst-SOC-OCV curve
  - b. parameter R0, R1 and Tau1
  - c. MHC test
  - d. DST test
  - e. General comments
- 4.3 EIG 11Ah LFP cell
  - a. Hyst-SOC-OCV curve
  - b. parameter R0, R1 and Tau1

c. MHC test
d. DST test
e. General comments
4.4 Kokam 30Ah cell
a. Hyst-SOC-OCV curve
b. parameter R0, R1 and Tau1
c. MHC test
d. DST test
e. General comments
4.5 Enerdel 15Ah cell
a. Hyst-SOC-OCV curve
b. parameter R0, R1 and Tau1
c. MHC test
d. DST test
e. General comments
4.6 Tests for Other Small Cells
4.7 Other Test Results
a. Dependency of Ah capacity on discharge Rate (nC)
b. Comparison of CCCV Discharge and CC Discharge
c. Scaling of Circuit Elements Based on Ah Capacity
5. Summary
References

1. Introduction

In electric vehicle modeling, a dynamic battery model is needed. A first-order transient response model is studied in this report. Tests are performed on lithium-ion cells of various chemistries to estimate the model parameters and to validate the model for dynamic test cycles. The first-order transient model is presented in Section 2 and the physical meaning of each parameter is discussed. Section 3 summarizes the test procedures and the test data for the various cells are given in Section 4. Dynamic test cycle results are also given in Section 4 to validate the model for nearly fixed SOC and over a wide SOC range. The summary and conclusions are given in Section5.

2. The First-Order Transient Response Model

Figure 1 illustrates the battery model proposed by PNGV/DOE in [1]. OCV (Open Circuit Voltage) is an ideal voltage source. R0 is the ohmic resistance. Rp and C are the polarized resistance and capacitance. 1/OCV is a capacitor which represents the open-circuit-voltage change due to discharge of the battery.

The first-order transient response model studied in this report, which is a variant of the PNGV model, is shown in Figure 2. Capacitor 1/OCV is eliminated and Vocv is a function of state-of-charge (SOC). Also, the parameters R0, R1 and C1 all vary with state-of-charge.

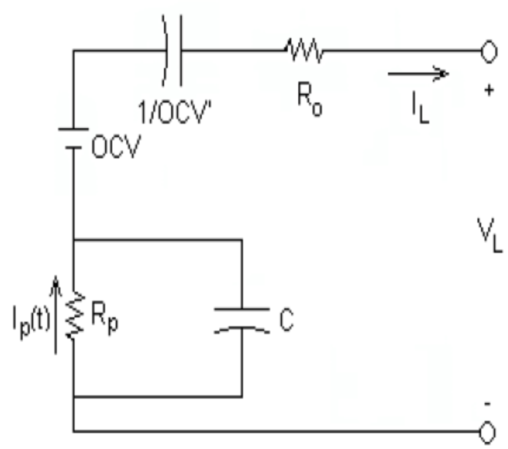

Figure 1 Model proposed by PNGV

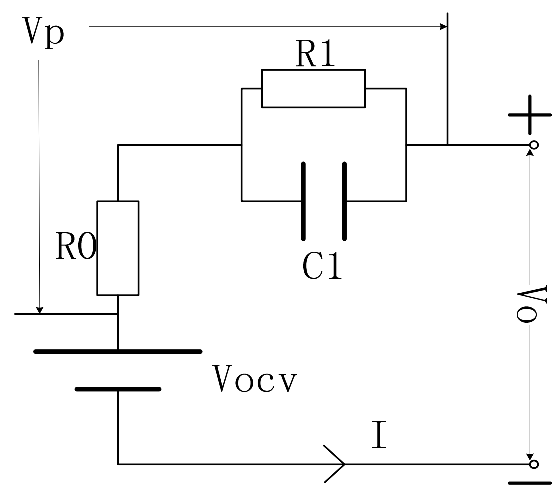

Figure 2 First-order transient response model

The output voltage V_c is given by

$$V_O = V_{OCV} + V_{R0} + V_{RC}$$

where

$$V_{OCV} = f(SOC)$$

$$V_{R0} = I(t) \times R0(SOC)$$

$$H(s) = \frac{V_{R0}(s)}{I(s)} = \frac{R1(SOC)}{R1(SOC) \times C1(SOC) \times s + 1}$$

$$SOC = SOC0 + \int_{t0}^{t} i(t)\,dt$$

The simulation flow diagram of the model in Matlab is illustrated in Figure 3. The model input is current $I(t)$, and the output is voltage $V_o(t)$. In this analysis, charging current is positive (I>0), and discharging current is negative (I<0). OCV, R0, R1 and C1 all vary with SOC and are given in lookup tables. The cell capacity and initial state-of-charge SOC0 are the initial conditions needed to run the simulation.

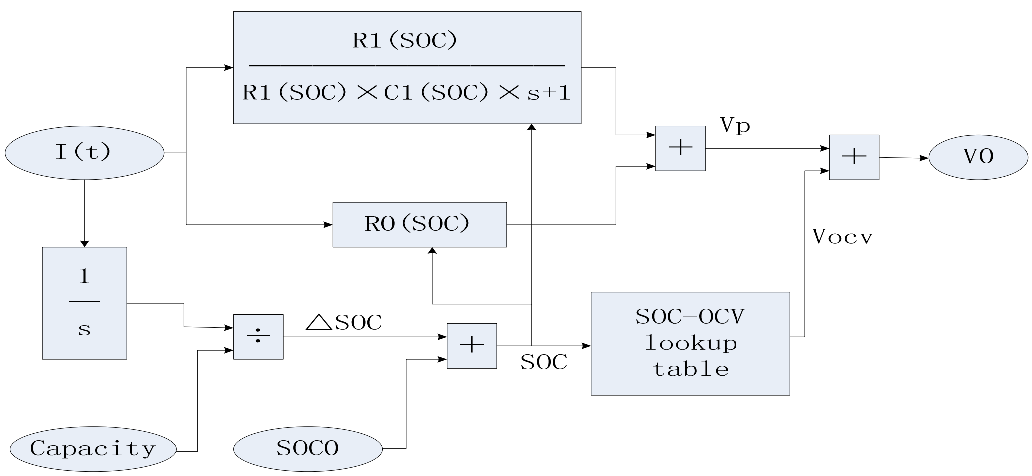

Figure 3 Simulation flow diagram of the Model

3. Test Procedures

In this section, the cells tested, battery tester utilized and data taken are discussed. The test procedures used to determine cell Ah capacity, open-circuit voltage curve hyst-SOC-OCV, and circuit element parameters are given. Finally the MHC and Dynamic Stress test cycles and data which are used to validate the model are presented. The DOE pulse HPPC tests are also performed on all cells.

3.1 Cells tested and test conditions

The cells tested are listed in Table 1. These cells were not all new. Some had been tested in previous studies [2, 3]. Photographs of the cells are shown in Figure 4.

Table 1: Tested cells

Cell Number	Manufacturer	chemistry Cathode/Anode	Voltage range (V)	Nominal Capacity(Ah)
1	Altairnano	NiMnO2/LiTiO	2-2.8	50
2	EIG	Nickel Cobalt/graphite	2.5-4.2	20
3	EIG	Iron phosphate/graphite	2-3.65	11
4	Kokam	NiCoMnO2/graphite	3.0-4.1	30
5	Enerdel	Ni MnO2/graphite	2.5-4.1	15
6	Quallion (SA type)	NiCo/graphite	2.7-4.2	1.2
7	Quallion (F type)	NiCo/graphite	2.7-4.2	2.5
8	K2	Iron phosphate/graphite	2-3.65	2.6

Figure 4: Tested cells

Battery tester: *Bitrode*

The tests were performed using a **Bitrode** battery tester which has voltage capability up to 50V and current capability of 400A in both charge and discharge. The *Bitrode*'s minimum data logging interval is 100ms. This is not good enough for pulse tests. For these tests, a ***National Instrument*** data logging setup was used and the data logging could be done to 1ms if needed.

3.2 Ah Capacity Tests and test procedure

:

a. Constant current (CC) charge: 1C rate, until voltage reaches the charging cut-off voltage;
b. Constant voltage (CV) charge: at charging cut-off voltage, until current reaches the cut-off current (about 1/10 the charging current);
c. Rest: 1 min;
d. Constant current (CC) discharge: 1C rate, until the voltage reaches the discharging cut-off voltage;
e. Constant voltage (CV) discharge: at discharging cut-off voltage, until current reaches the cut-off current C/10 or the lowest A of the tester (1A);
f. Rest: 1 min;
g. Repeat the steps above for 3 cycles.

The Ah capacity of the third cycle is taken as the Ah capacity of the cell.

3.3 Hyst-SOC-OCV Curve test

a. SOC Definition

In the capacity test, SOC=1 is defined when a cell is at the end of the CV charge step and reaches the cut-off current. From the point (SOC=1), the net discharge Ah is Cap_dch and

$$\mathrm{SOC} = 1 - \frac{\mathrm{Cap\_dch}}{Capacity}$$

b. Hyst-SOC-OCV curve

From previous testing, it was found that there is a hysteresis effect on the open-circuit voltage when we charge or discharge a battery over a long time (say 1C charge/discharge) even when the polarization (Vp) illustrated in Figure 2 is removed. A C/10 rate test cycle is performed to get the hyst-SOC-OCV curve. The hyst-OCV is

$$V_{hyst-ocv} = V_{C/10} - I \times (R0 + R1)$$

where $V_{C/10}$ is the charge/discharge curve. The charge current is in the positive direction, and the discharge current is in the negative direction.

3.4 Circuit Elements Test

When using a single pulse to estimate the circuit elements R0, R1 and C1, the parameters R1 and C1 are difficult to determine with good precise. Sequences of step pulses contain more information than a single pulse. In order to distinguish the difference of these elements between charging and discharging, both charge step pulses and discharge step pulses are included in the sequences.

The test profiles of charge step pulses are shown in Table 2 and Figure 5. The amplitudes of discharge step pulses are the same as charge step pulses. Both charge step pulses and discharge step pulses are done at SOC=0.1, 0.3, 0.5, 0.7, 0.9. There is a 30min rest before the start of each set of step pulse profiles.

3.5 Hybrid Pulse Power Characterization (HPPC) Test

HPPC test is specified by the USABC [4]. The HPPC test profile is shown in Table 3 and Figure 6. It is also done at SOC=0.1, 0.3, 0.5, 0.7, 0.9, and a 30min rest is required before starting the test. Using the HPPC test results, the power capability of the cell at 95% voltage-efficiency can be calculated.

The power at specific voltage-efficiency (V_0/V_{ocv}) is

$$P = I \times V_0 = \frac{(V_0 - V_{ocv})}{R} \times V_0$$

$$= \left(\frac{V_0}{V_{ocv}} - 1\right) \times V_0 \times \frac{V_{ocv}}{R}$$

$$= -\left(1 - \frac{V_0}{V_{ocv}}\right) \times V_{ocv}^2 \times \frac{\frac{V_0}{V_{ocv}}}{R}$$

$$= -(1 - EF) \times \frac{EF \times V_{ocv}^2}{R}$$

Where R uses the 10s discharge resistance R_{10s} that can be obtained in HPPC test. EF is the voltage efficiency

$$EF = \frac{V_0}{V_{ocv}}$$

When the voltage efficiency is 95%, the discharge power is

$$P_{95\%} = -(1 - EF) \times \frac{EF \times V_{ocv}^2}{R_{10s}} = -(1 - 0.95) \times \frac{0.95 \times V_{ocv}^2}{R_{10s}} = -0.0475 \times \frac{V_{ocv}^2}{R_{10s}}$$

Table 2: Charge Step Pulses Test Profile:

Current	Step time(sec)	Accumulated time(sec)
5C	8	8
3.5C	10	18
2C	12	30
6C	3	33

Table 3: HPPC Test Profile:

Current	Step time(sec)	Accumulated time(sec)
-5C	10	10
0	40	50
4C	10	60

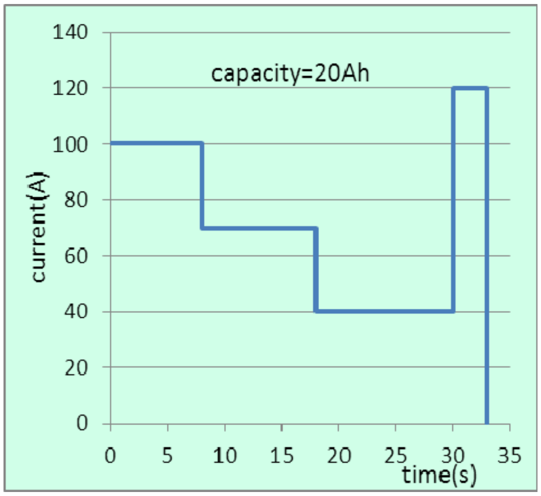

Figure 5 Charge Step Pulses Test Profile

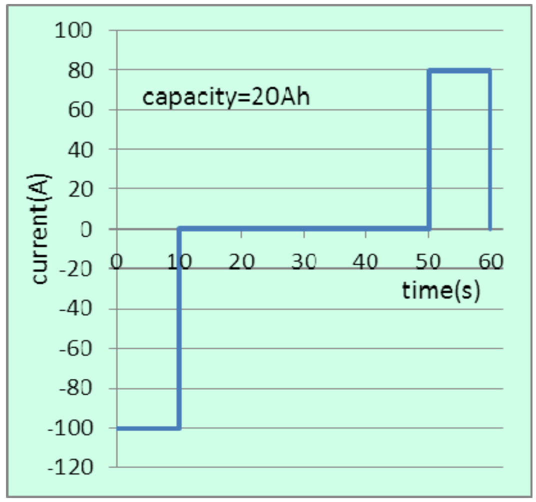

Figure 6 HPPC Test Profile

3.6 MHC Test

The MHC test profile is shown in Table 4 and Figure 7. It is given in power rather than current as was done for the case for the HPPC test. The power of the pulse is given as N times $P_{95\%}$. The object of MHC test is to validate the First-Order Transient Response Model at a nearly fixed state-of-charge, say SOC=0.5. We can evaluate the model by comparing the actual cell voltage with the output voltage calculated using the model. If they match well, then the model is validated for a fixed SOC.

Table 4: MHC Pulses Test Profile

N times the $P_{95\%}$	Step time(sec)	Accumulated time(sec)
0	8	8
-2.85 (discharge)	5	13
-1.43	10	23
1.71 (charge)	12	35
2.57	5	40

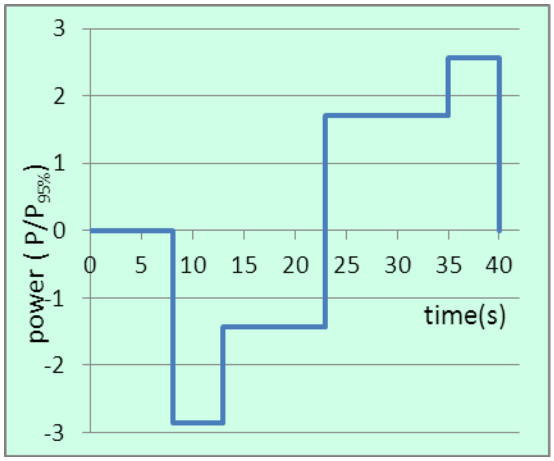

Figure 7 MHC Pulses Test Profile

3.7 Dynamic Stress Test

The MHC test is to validate the model at a fixed state-of-charge; the Dynamic Stress Test (DST) is used to validate the model over a wide SOC range. One DST cycle profile is shown in Table 5 and Figure 8. DST test cycle was also proposed by USABC [4]. Before the Dynamic Stress Test, a cell is charged to SOC=1. Then DST cycles are performed on the cell until it reaches the discharge cut-off voltage.

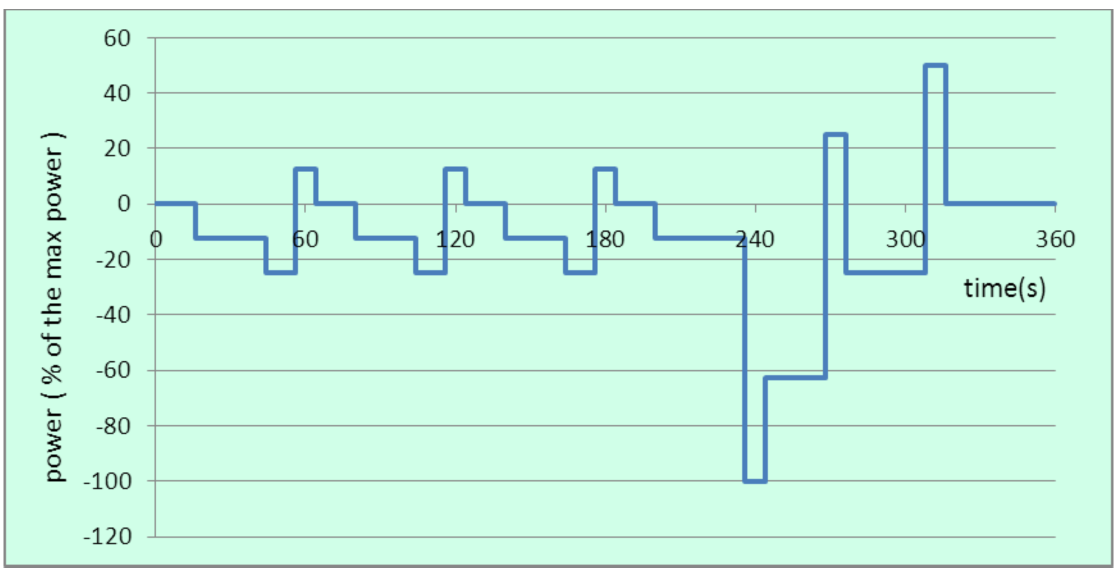

Figure 8 Dynamic Stress Test Profile

4. Test Results and Model Validation

The characteristics of the various cells that were tested are given in table 6, including Ah capacity, weight, R_{10s} and specific power $P_{95\%}$ (W/kg) at SOC=0.5, and specific energy (Wh/kg). The hyst-SOC-OCV curves and the circuit element parameters as they apply to the various cells are discussed later in this section. For each cell, the first-order transient response model is validated by comparing the model's predictions of output voltages for the MHC and DST cycles to the experimental data.

Table 5: Dynamic Stress Test Profile

Power (%of the max power)*	Step time(sec)	Accumulated time(sec)
0	16	16
-12.5 (discharge)	28	44
-25	12	56
12.5 (charge)	8	64
0	16	80
-12.5	24	104
-25	12	116
12.5	8	124
0	16	140
-12.5	24	164
-25	12	176
12.5	8	184
0	16	200
-12.5	36	236
-100	8	244
-62.5	24	268
25	8	276
-25	32	308
50	8	316
0	44	360

*the maximum power is 120W/kg

Table 6: Summary of the cell characteristics

Cell	Capacity (Ah)	Weight (g)	Specific $P_{80\%}$ (W/kg) (SOC=0.5)	Specific energy (Wh/kg)	R_{10s} (mΩ) (SOC=0.5)
Altairnano 50	50.8	1596	118.4	62.7	1.4
EIG NiCo	18.3	409.5	335.5	146.5	4.9
EIG LFP	10.1	324.5	326.7	83.2	4.9
Kokam	28.2	785.3	274.9	117.2	3.0
Enerdel	14.3	444.8	562.0	82.3	2.5
Quallion (SA)	1.0	43.4	254.2	----	62.1
Quallion (F)	1.8	47	156.7	----	90.4
K2	2.2	82.8	177.0	----	35.3

4.1 Altairnano 50Ah Cell

a. Hyst-SOC-OCV curve

The hyst-SOC-OCV curve for the Altairnano 50Ah cell is shown in Figure 9. The CH_C/10 curve and the DCH_C/10 curve are the C/10 rate charge and discharge curves. The OCV-CH curve is the result of the subtraction of CH_C/10 and V_p, the polarization voltage for the C/10 current. The OCV-DCH curve is the result of the sum of DCH_C/10 and V_p.

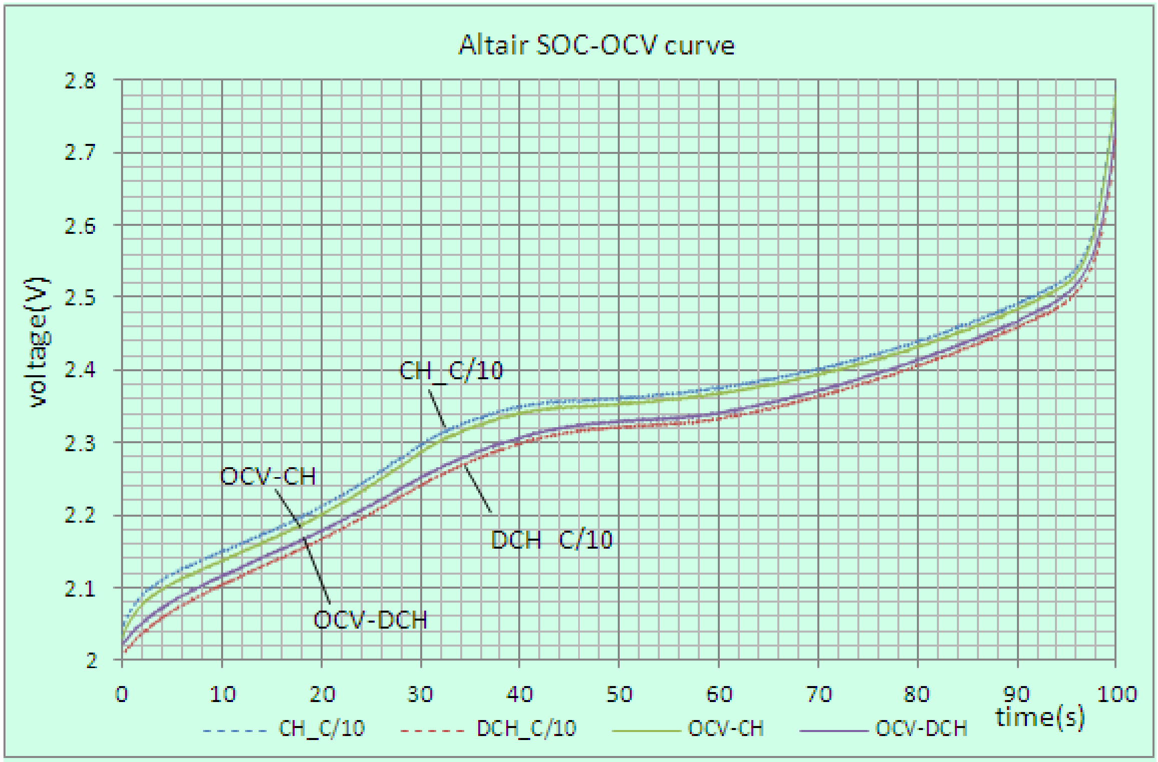

Figure 9 Altair 50Ah hyst-SOC-OCV Curve

b. Parameters R0, R1 and Tau1

The circuit elements R0, R1 and Tau1 are listed in Table 7. Tau1 is the time constant. $Tau1 = R1 \times C1$. The parameters in "DCH" columns are estimated from discharge step pulses and the parameters in "CHR" columns are estimated from charge step pulses.

c. MHC test

The MHC test currents, test voltages and the estimated output voltages of the model are shown in Figure 10. The estimated voltage fits the test voltage well.

d. DST test

Since the DST cycles are mainly composed of discharge pulses, the circuit elements "DCH" and the hyst-SOC-OCV curve - the "OCV-DCH" were used in the simulation calculations.
The dynamic stress test current, test voltage and the estimated output voltage of the model are shown in Figure 11. The maximum power step for this cell is 240W. Figure 12 is a zoom-in view of a center part of the DST cycle (Figure 11). The estimated output voltages fit the test voltages well. A zoom-in view of the first 1200s is shown in Figure 13. The biggest error is 50mV, which occurs at SOC near 1 and at high current. At 600s, the estimated SOC is 0.95, and the model works well after that time. At the end of DST cycles, SOC is 0.2. Thus, the first-order transient response model can be applied to simulate a lithium titanium battery dynamically in 0.2-0.95 SOC range.

Table 7: Altair 50Ah circuit element parameters

SOC	DCH			CHR		
	R0(mΩ)	R1(mΩ)	Tau1(sec)	R0(mΩ)	R1(mΩ)	Tau1(sec)
0.1	1.97	0.60	25	1.40	0.49	13
0.3	1.54	0.68	32	1.22	0.56	21
0.5	1.23	0.31	19	1.13	0.33	19
0.7	1.17	0.37	23	1.07	0.40	24
0.9	1.13	0.45	24	1.04	0.55	31

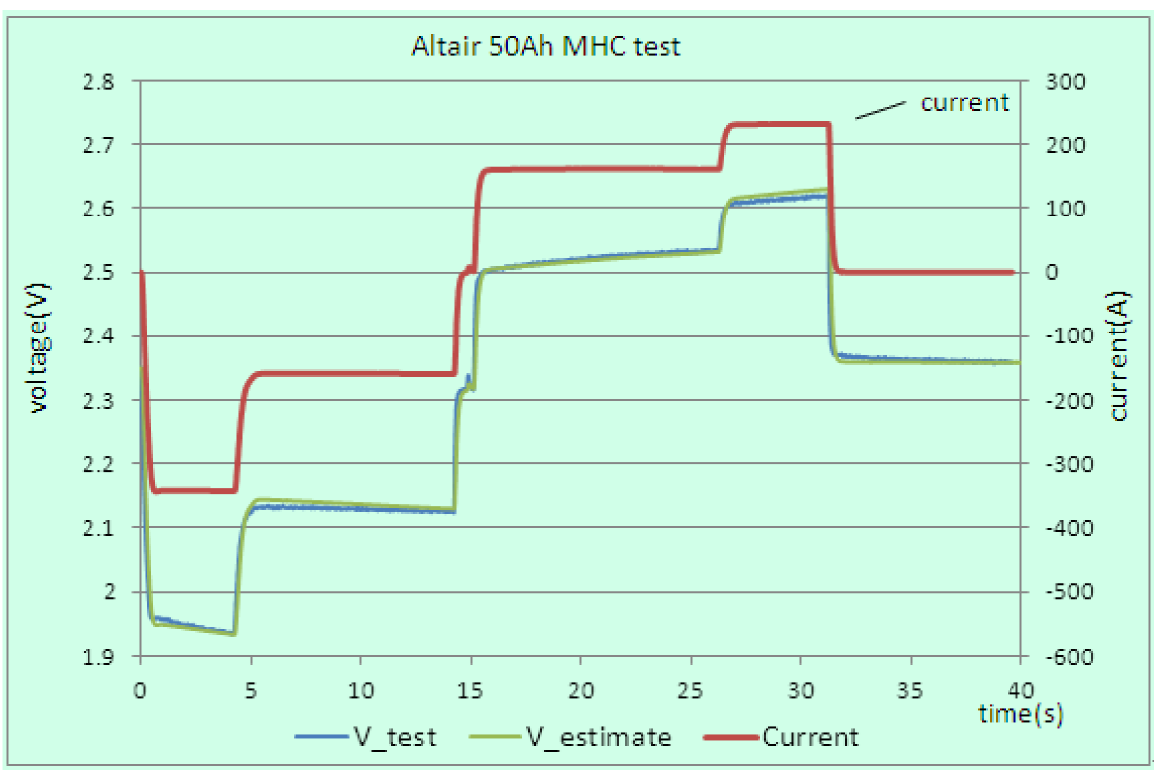

Figure 10: Altair 50Ah MHC

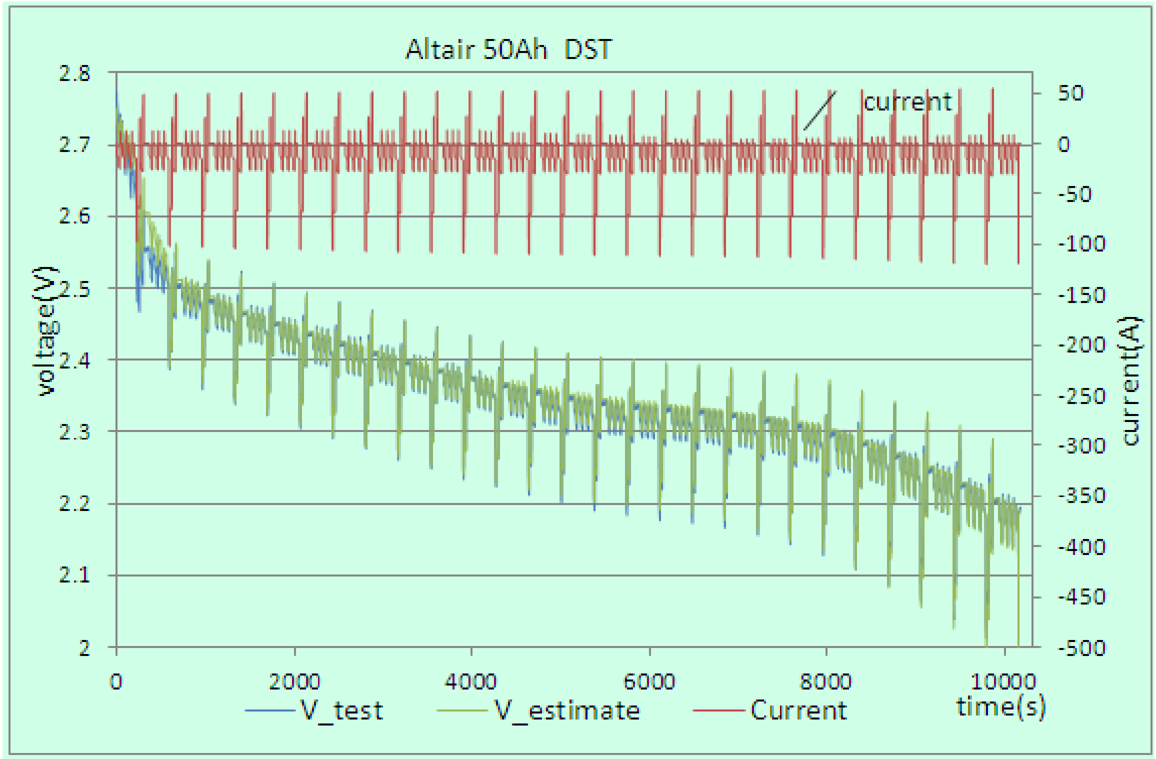

Figure 11 Altair 50Ah DST Simulation

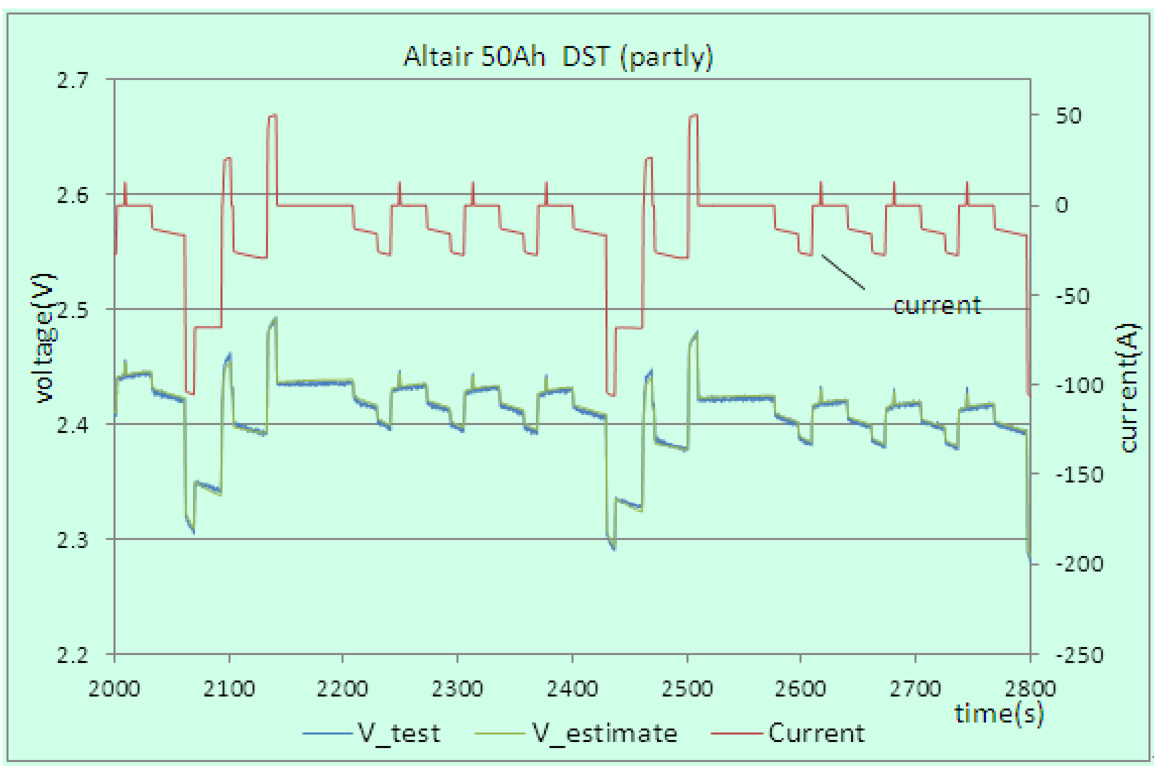

Figure 12 Altair 50Ah DST simulation(part- zoom in)

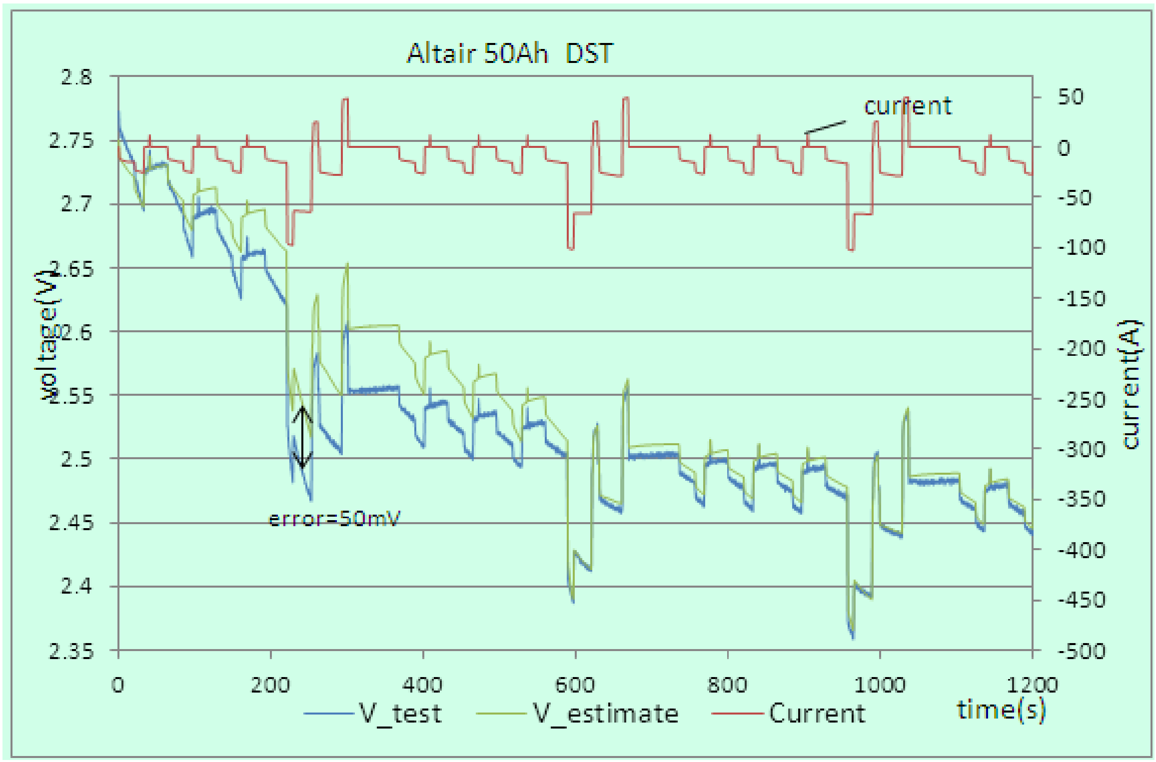

Figure 13 Altair 50Ah first 1200s of the DST simulation

e. General comments

An open-circuit voltage hysteresis exists for a lithium titanium battery (see Figure 9). The hysteresis is significant for the determination of SOC from the open-circuit voltage. The differences between the estimated “CHR” circuit elements and the “DCH” circuit elements are in general not large, but they are likely significant in terms of their effect on the predicted voltages from the model. The discharge parameters are larger than the charge ones, but they have the same tendencies.

In the MHC test, the estimated voltage fits the test voltage well. The first-order transient response model can be applied to simulate a lithium titanium battery dynamically at a fixed SOC, and the error can be ignored. In the DST test, the estimated output voltage fits the test voltage quite well. The biggest error of 50mV occurs at high SOC near full charge. There are two reasons for this error. One is that the circuit elements are valid in the 0.1-0.9 SOC range, not beyond this range. When the SOC is outside the 0.1-0.9, MATLAB extrapolates the parameters. The real parameters of the cell are higher than the extrapolated ones. The other reason is that the polarization is much higher at high currents, caused by higher concentration gradient in the electrode. The first-order transient response model can be applied to simulate a lithium titanium battery dynamically in 0.2-0.95 SOC range.

4.2 EIG 20Ah NiCo cell

a. Hyst-SOC-OCV curve

The hyst-SOC-OCV curve of the EIG NiCo cell is shown in Figure 14.

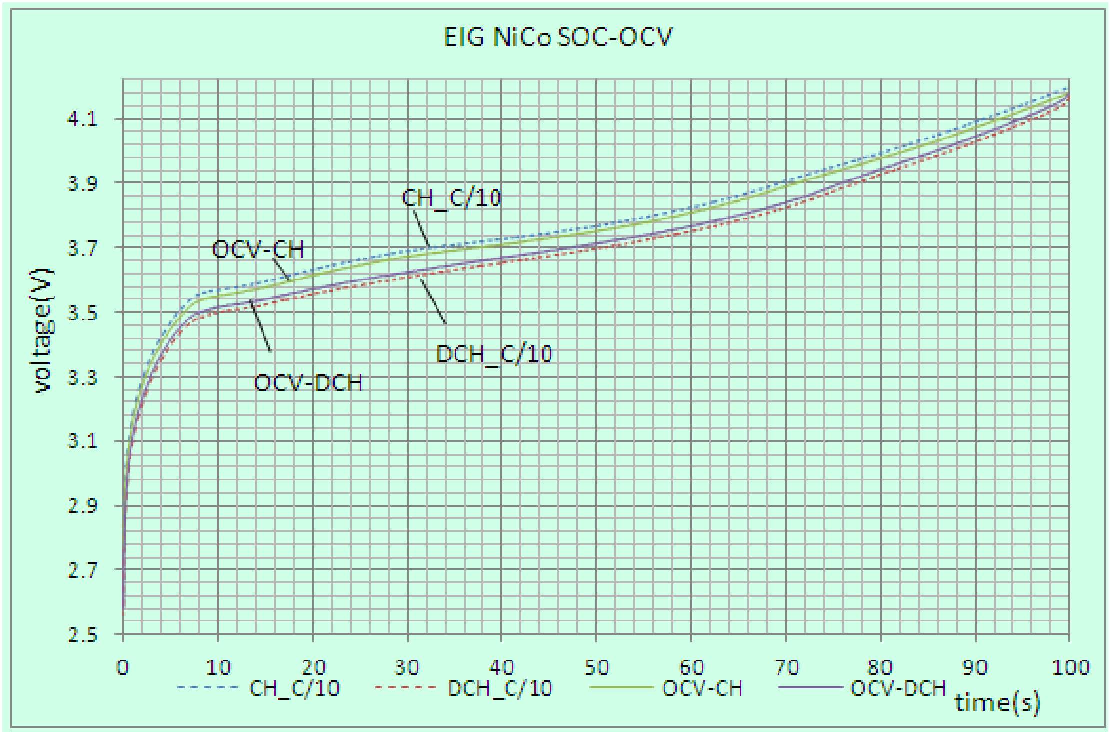

Figure 14 EIG NiCo hyst-SOC-OCV curve

b. Parameters R0, R1 and Tau1

The circuit elements *R0, R1* and *Tau1* are listed in Table 8.

Table 8: EIG 20Ah NiCo parameters

SOC	DCH			CHR		
	R0(mΩ)	R1(mΩ)	Tau1(sec)	R0(mΩ)	R1(mΩ)	Tau1(sec)
0.1	5.57	4.76	42	4.94	3.65	37
0.3	4.64	2.97	41	4.53	3.01	43
0.5	4.30	3.01	43	4.25	3.18	44
0.7	4.15	3.39	42	4.30	4.00	53
0.9	4.14	3.59	43	4.38	4.13	54

c. MHC test results

The MHC test current, test voltage and the estimated output voltage of the model are shown in Figure 15.

d. DST test

The dynamic stress test current, test voltage and the estimated output voltage of the model are shown in Figure 16. Figure 17 is the zoom-in view of the last three DST cycles. The maximum power step for this cell is 160W. The estimated output voltages fit the test voltage well, except at the end of the last two DST cycles (SOC near 0). The biggest error is 200mV, and the SOC is 0.02 at that time. The estimated voltages fit well until 9400s (SOC = 0.108). When SOC is greater than 0.9, there's also a significant error.

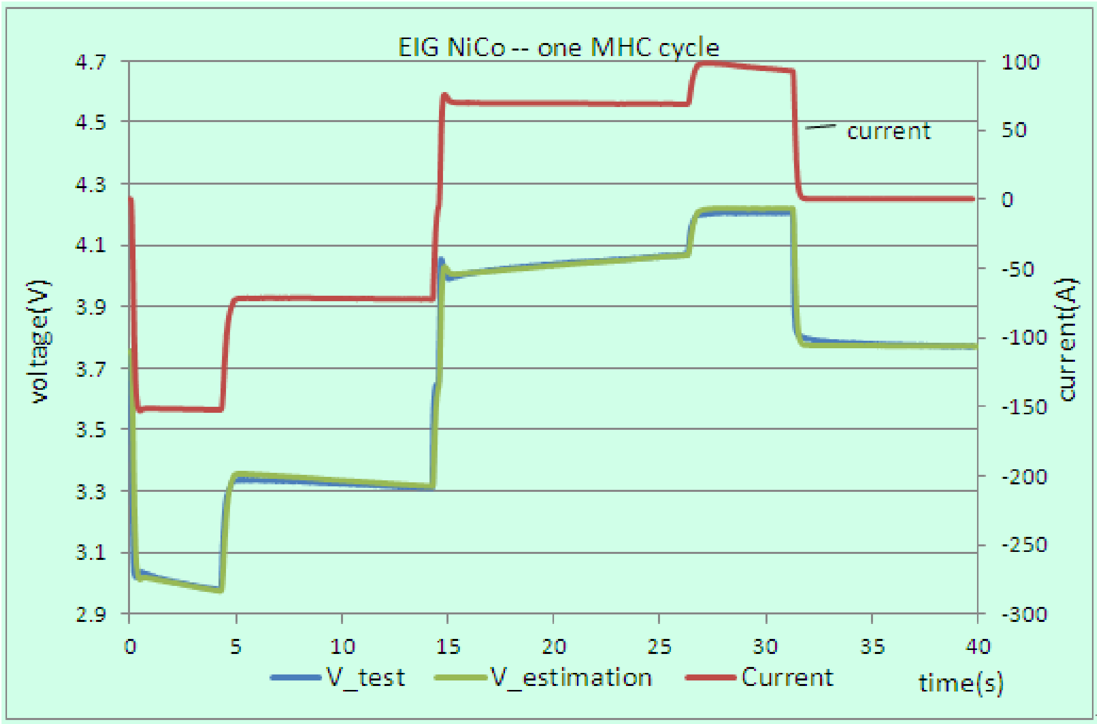

Figure 15 EIG NiCo MHC Simulation

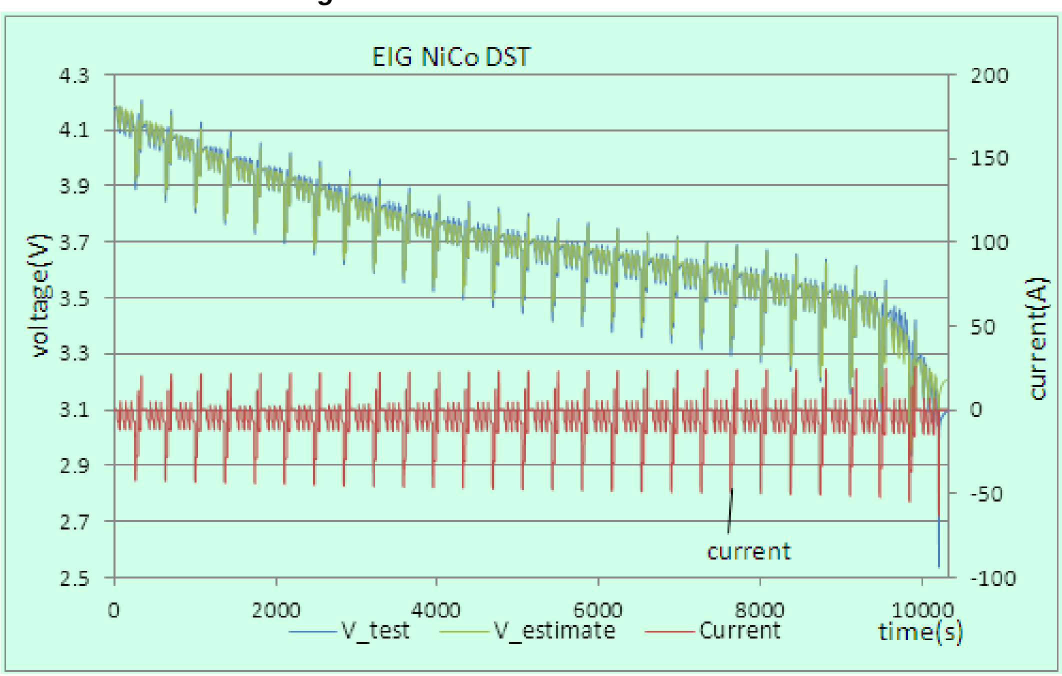

Figure 16 EIG NiCo DST simulation

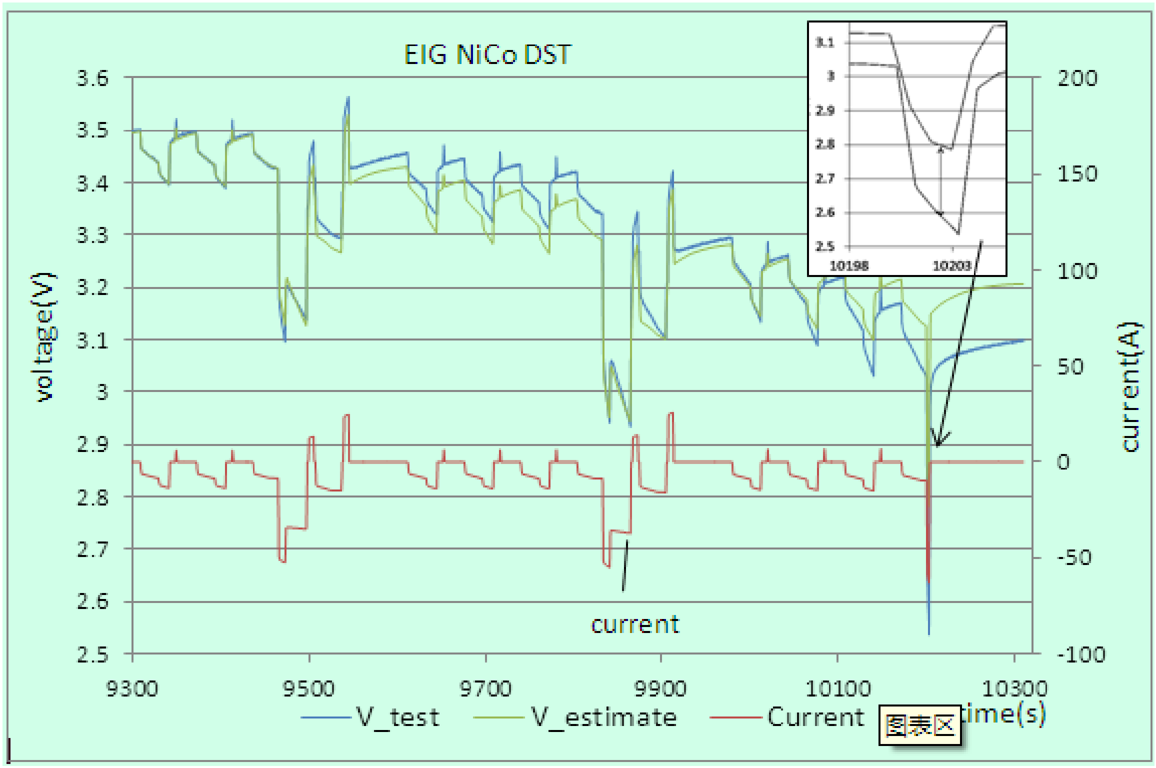

Figure 17 EIG NiCo last three DST cycles

e. General comments

An open-circuit voltage hysteresis exists for a lithium nickel cobalt battery (see Figure 14). The hysteresis makes determination of SOC from OCV difficult for this chemistry. The estimated "CHR" circuit elements and the "DCH" circuit elements are given in Table 8. The differences between the parameters for charge and discharge are relatively small for this chemistry.

In the MHC test, the estimated voltage fits the test voltage well. The first-order transient response model can be applied to simulate a lithium nickel cobalt battery dynamically at a fixed SOC, and the errors can be ignored. For the DST cycles, the estimated output voltage also fits the test voltage well. The biggest error, that is 200mV, occurs when SOC is 0.02. The first-order transient response model can be used for a lithium nickel cobalt battery dynamically in the 0.1-0.9 SOC range.

4.3 EIG 11Ah LFP cell

a. Hyst-SOC-OCV curve

The hyst-SOC-OCV curve of EIG lithium iron phosphate cell is shown in Figure 18.

b. Parameters R0, R1 and Tau1

The circuit elements R0, R1 and Tau1 are listed in Table 9.

c. MHC test

The MHC test current, test voltage and the estimated output voltage of the model are shown in Figure 19.

d. DST test

The dynamic stress test current, test voltage and the estimated output voltage of the model are shown in Figure 20. Figure 21 is the zoom-in view of the last two DST cycles. The maximum power step for this cell is 160W. The estimated output voltage fits the test voltage well, except at both ends of the test (SOC near 0 and 1). The biggest error is almost 500mV at the end of the test (SOC = 0.05). Until 3900s, the estimated voltage fits well, and SOC is 0.23 by then. When SOC is higher than 0.85 (before 700s), there's also a significant error.

Table 9 EIG 11Ah LFP cell parameters

SOC	DCH			CHR		
	R0(mΩ)	R1(mΩ)	Tau1(sec)	R0(mΩ)	R1(mΩ)	Tau1(sec)
0.1	4.32	7.51	52	4.11	4.52	28
0.3	4.01	3.69	27	3.72	2.69	23
0.5	3.92	2.71	21	3.96	2.93	22
0.7	4.12	3.28	21	3.92	2.59	19
0.9	3.86	2.76	20	4.12	6.49	42

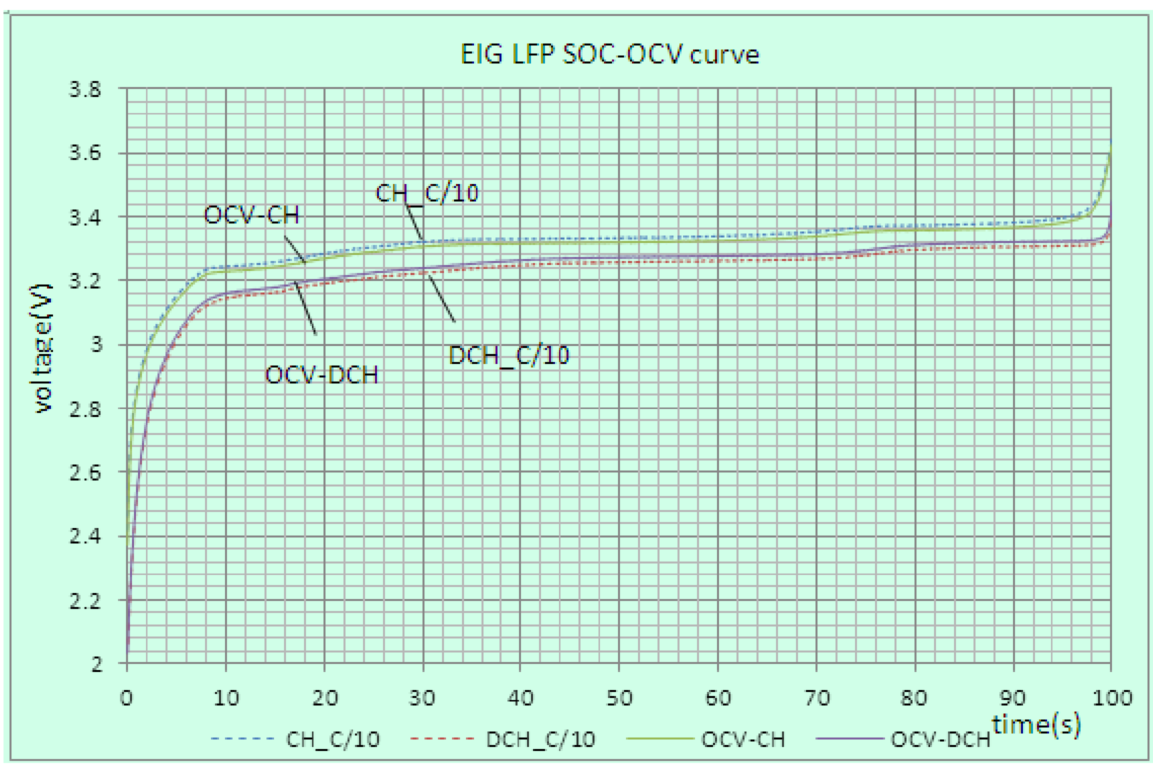

Figure 18 EIG LFP Hyst-SOC-OCV curve

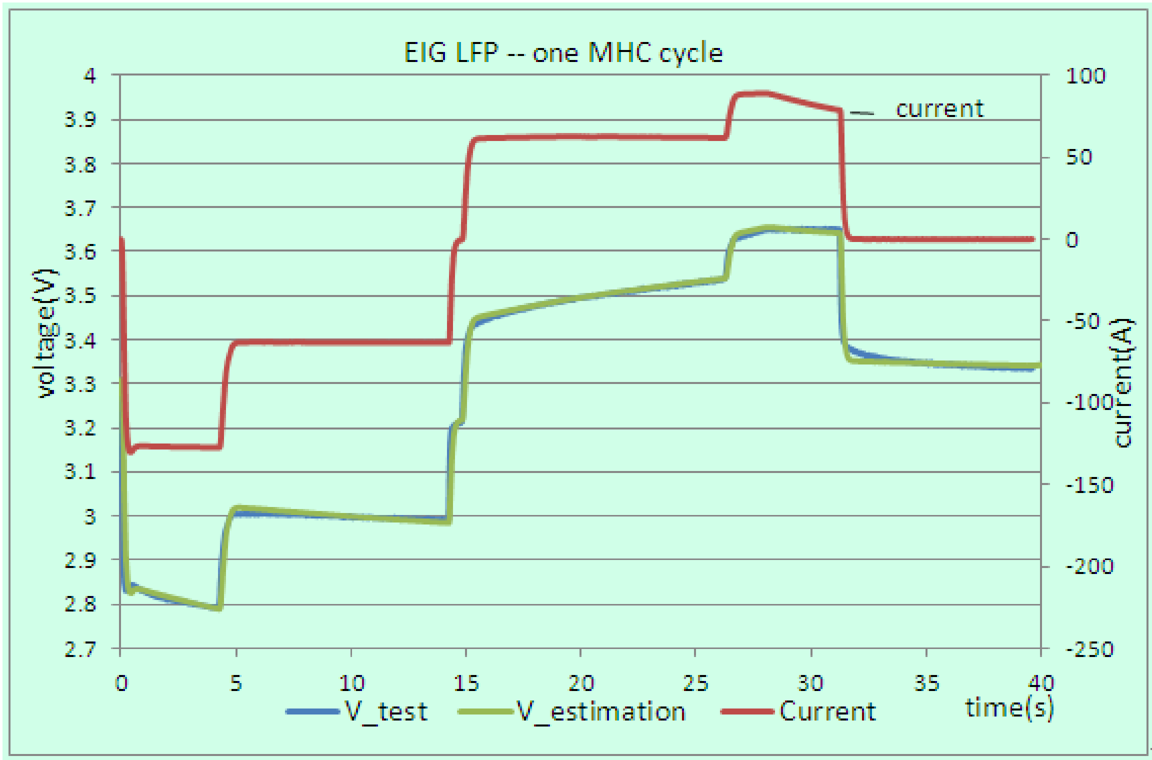

Figure 19 EIG LFP MHC Simulation

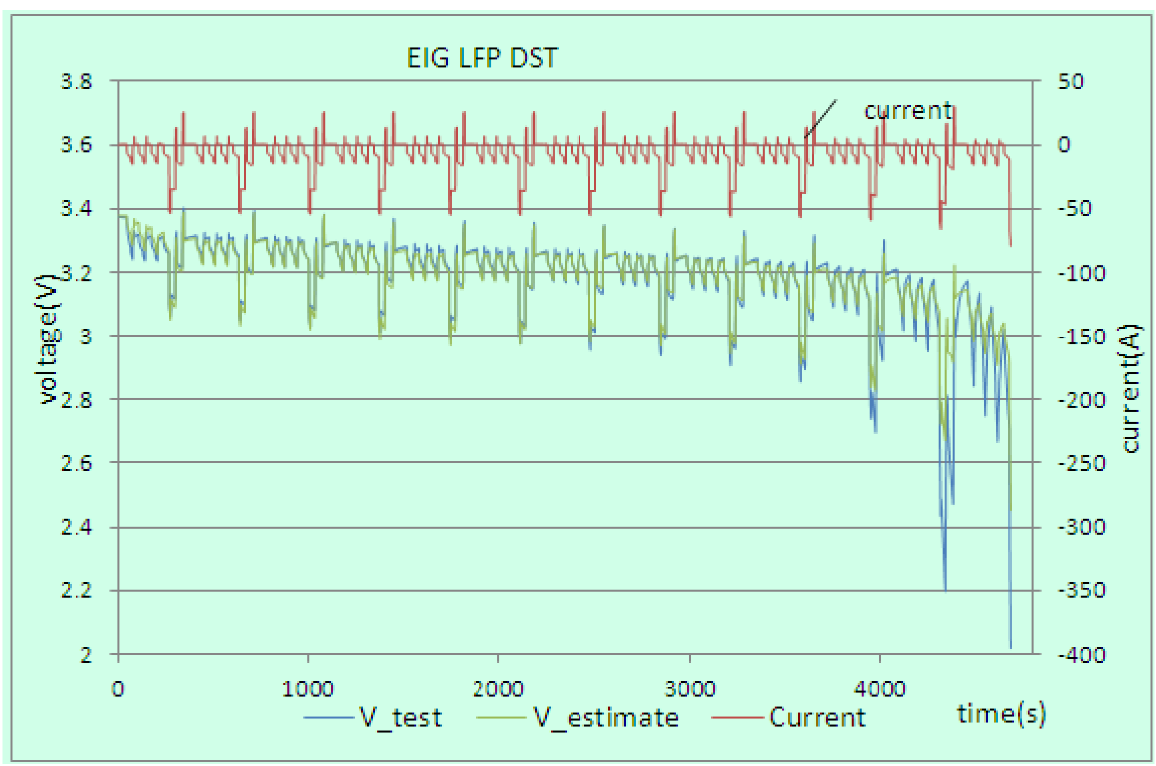

Figure 20 EIG LFP DST simulation

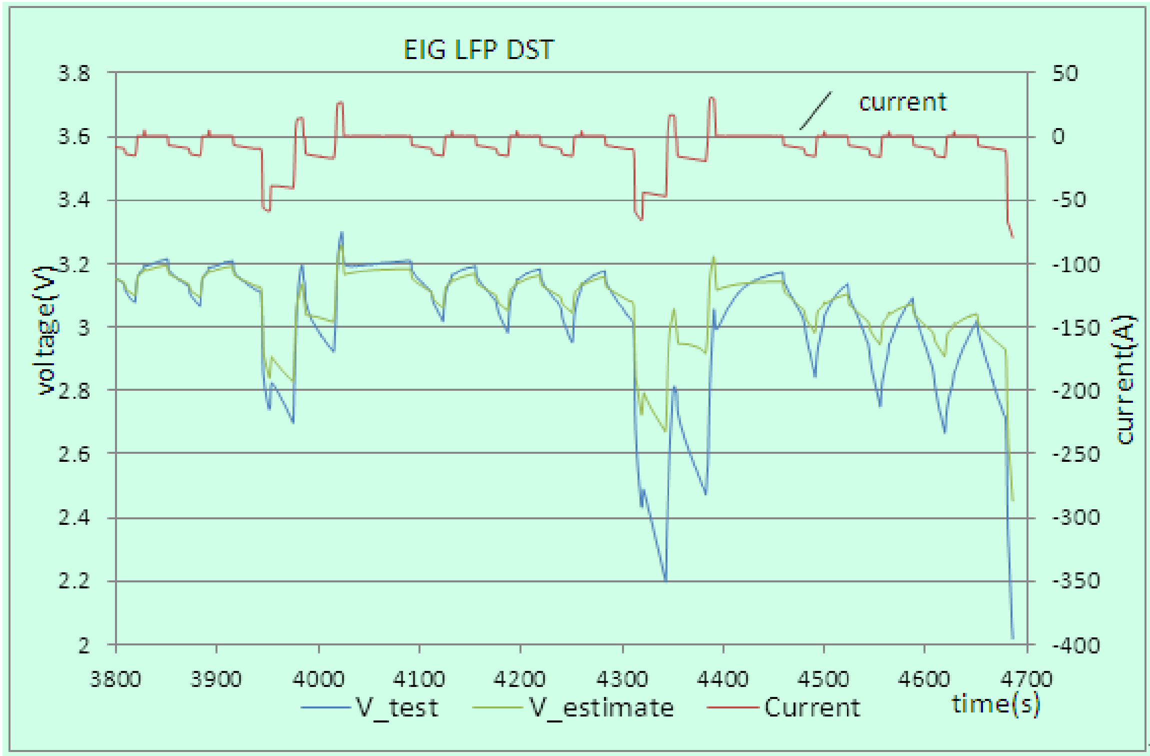

Figure 21 EIG LFP last two DST cycles

e. General comments

An open-circuit voltage hysteresis exists for a lithium iron phosphate battery (see Figure 18). This hysteresis makes determination of SOC particularly difficult for this chemistry. The estimated "CHR" circuit elements and the "DCH" circuit elements given in Table 9 show large variations with SOC and charge/discharge.

In the MHC test, the estimated voltage fits the test voltage well. The first-order transient response model can be applied to simulate a lithium iron phosphate battery dynamically at a fixed SOC. In the DST test, the estimated output voltage fits the test voltage well in the 0.23-0.85 SOC range.

4.4 Kokam 30Ah cell

a. Hyst-SOC-OCV curve

The Hyst-SOC-OCV curve of Kokam lithium nickel cobalt manganese cell is shown in Figure 22.

b. Parameters R0, R1 and Tau1

The circuit elements R0, R1 and Tau1 the cell are listed in Table 10.

c. MHC test

The MHC test current, test voltage and the estimated output voltage of the model are shown in Figure 23.

d. DST test

The dynamic stress test current, test voltage and the estimated output voltage of the model are shown in Figure 24. Figure 25 is the zoom-in view of the last three DST cycles. The maximum power step for this cell is 160W. The estimated output voltage fits the test voltage well. The biggest error is about 150mV at the end of the test where the SOC is 0.06. There's also a significant error when SOC is higher than 0.94 (before 500s).

Table 10 Kokam 30Ah cell parameters

SOC	DCH			CHR		
	R0(mΩ)	R1(mΩ)	Tau1(sec)	R0(mΩ)	R1(mΩ)	Tau1(sec)
0.1	3.70	4.19	16	2.85	2.30	31
0.3	2.95	1.99	30	2.71	1.91	36
0.5	2.59	1.54	30	2.58	1.91	40
0.7	2.48	1.94	34	2.59	2.40	49
0.9	2.43	1.96	35	2.69	2.26	52

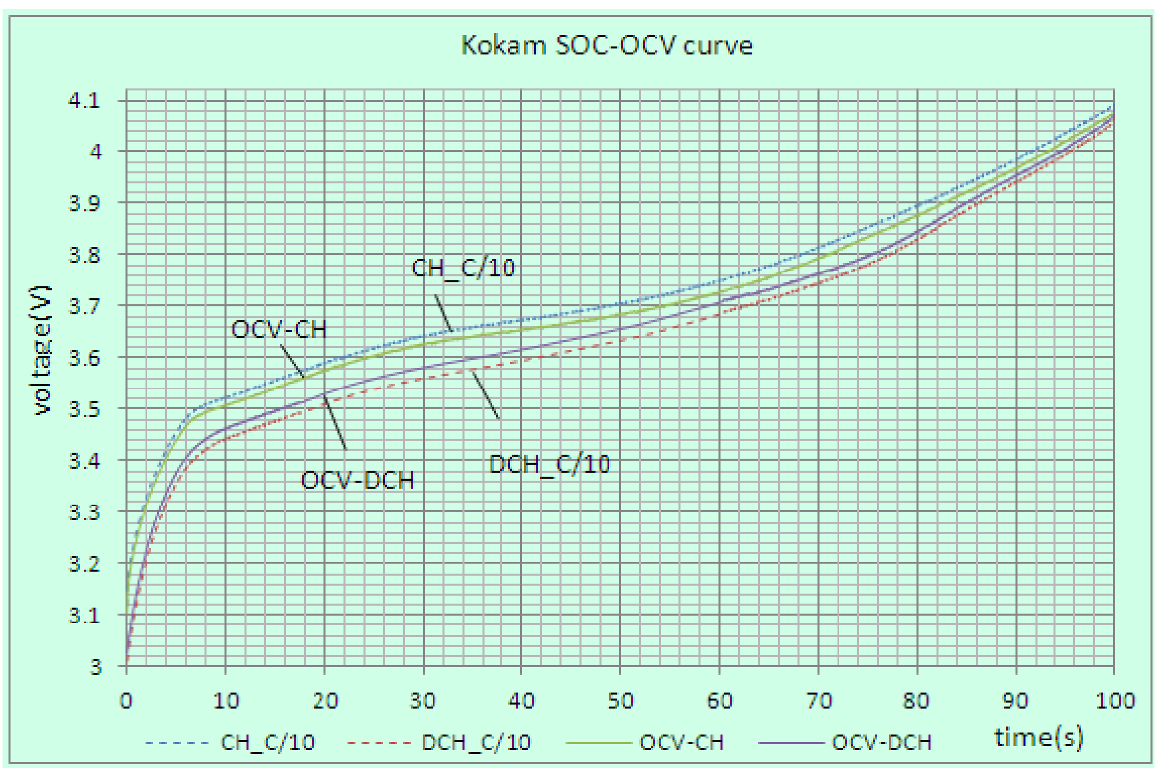

Figure 22 Kokam Hyst-SOC-OCV curve

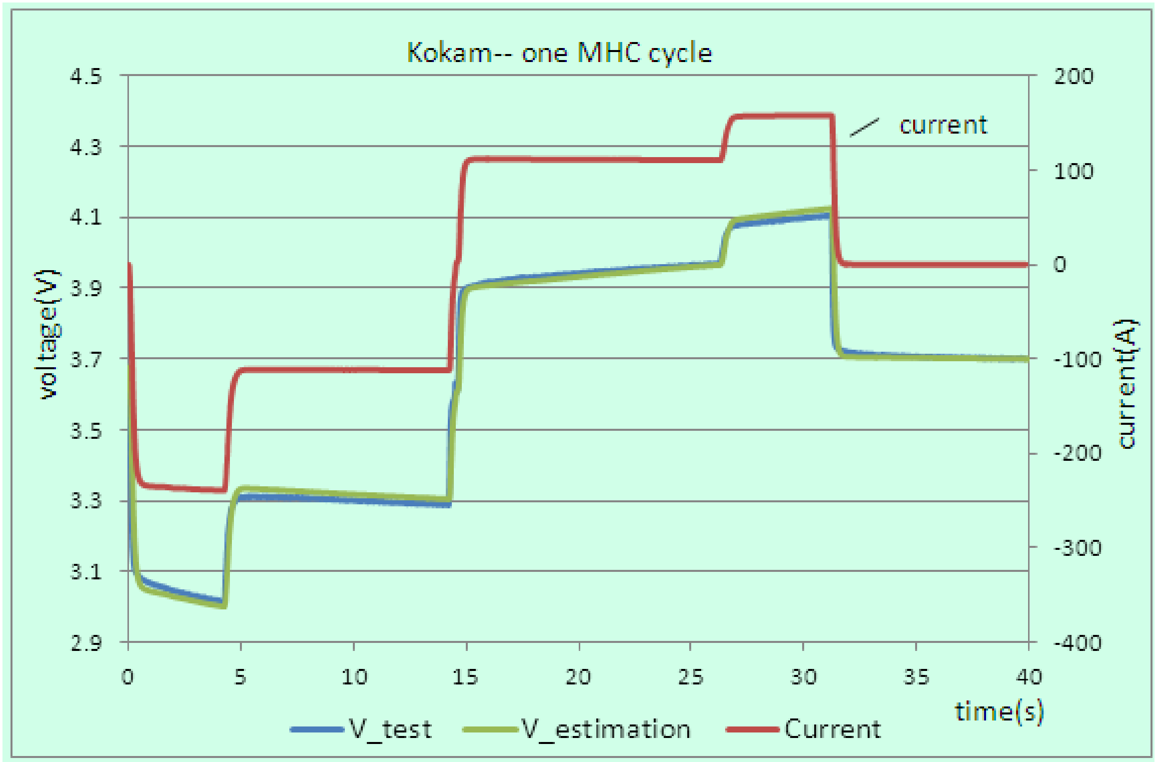

Figure 23 Kokam MHC Simulation

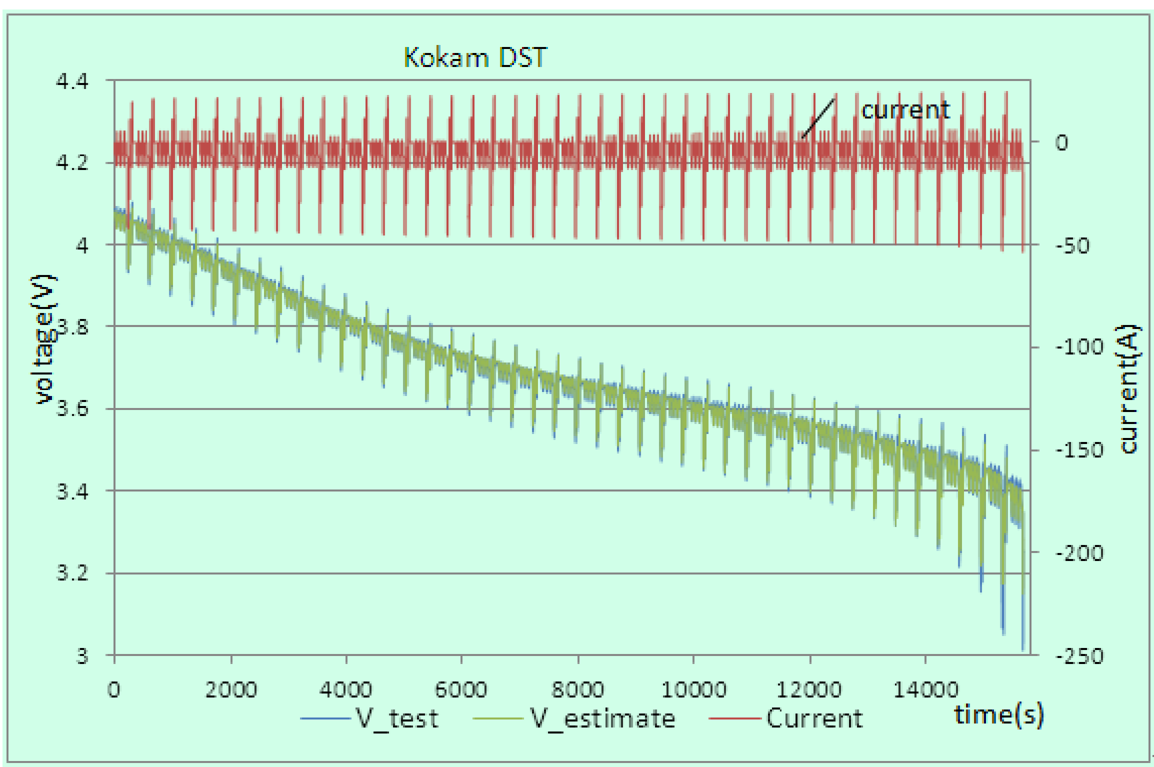

Figure 24 Kokam DST Simulation

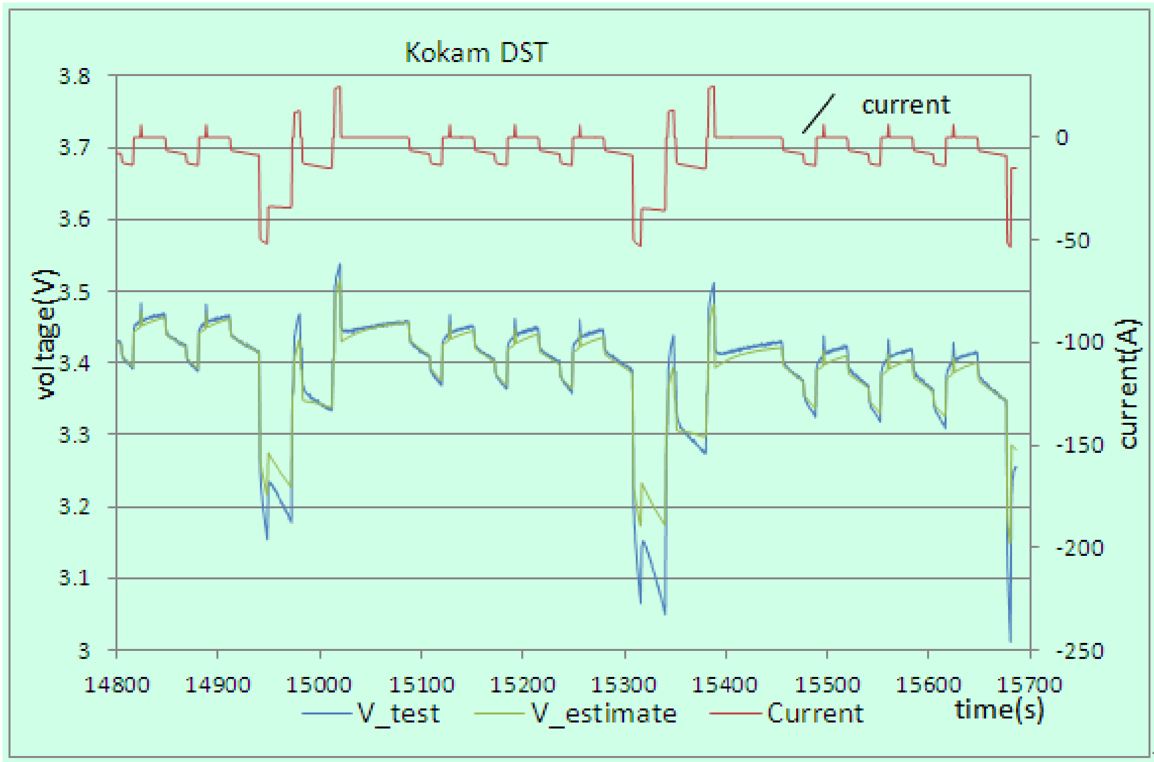

Figure 25 Kokam last three DST cycles

e. General comments

An open-circuit voltage hysteresis exists for a Kokam lithium nickel cobalt manganese battery (see Figure 22). This hysteresis makes determination of SOC difficult for this chemistry. From Table 10, it is seen that the estimated “CHR” circuit elements R0 and R1 are little bigger than the “DCH” circuit element at higher SOC, and the estimated “DCH” circuit elements R0 and R1 are much bigger than the “CHR” circuit element at 0.1SOC. This is also a reflection of the SOC-OCV curve, which is much steeper at low state-of-charge.

In the MHC test, the estimated voltage fits the test voltage well. The first-order transient response model can be applied to simulate a lithium nickel cobalt manganese battery dynamically at a fixed SOC. In the DST test, the estimated output voltage fits the test voltage well in the 0.13~0.94 SOC range. Hence the first-order transient response model can be used to model the dynamics of a lithium nickel cobalt manganese battery.

4.5 Enerdel 15Ah cell

a. Hyst-SOC-OCV curve

The Hyst-SOC-OCV curve of Enerdel lithium nickel manganese cell is shown in Figure 26.

b. Parameters R0, R1 and Tau1

The circuit elements R0, R1 and Tau1 are listed in Table 11.

c. MHC test

The MHC test current, test voltage and the estimated output voltage of the model of Enerdel lithium nickel manganese cell are shown in Figure 27.

d. DST test

The dynamic stress test current, test voltage and the estimated output voltage of the model are shown in Figure 28. Figure 29 is a zoom-in view of about four DST cycles in the middle of the test. Figure 30 is a zoom-in view of the last three cycles of the test (SOC = 0.07). The maximum power step for this cell is 160W. The estimated output voltage fits the test voltage well if the test current is small, but when the test current is high, the errors are large as shown inside the ellipse in Figure 29.

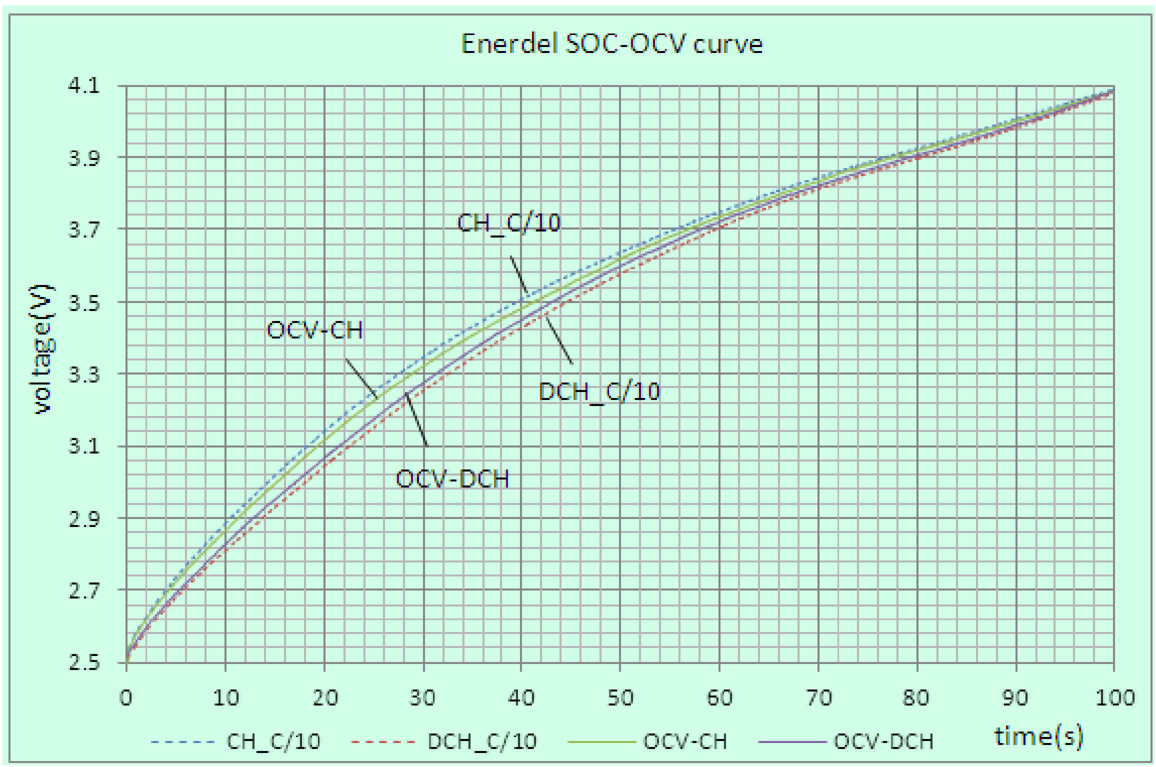

Figure 26: Enerdel Hyst-SOC-OCV Curves

Table 11: Enerdel 15Ah cell parameters

SOC	DCH			CHR		
	R0(mΩ)	R1(mΩ)	Tau1(sec)	R0(mΩ)	R1(mΩ)	Tau1(sec)
0.1	2.40	9.19	71	2.24	8.42	74
0.3	1.97	6.58	77	1.91	5.99	72
0.5	1.80	4.20	61	1.79	4.30	62
0.7	1.73	3.33	53	1.73	3.36	54
0.9	1.66	3.52	59	1.63	3.13	54

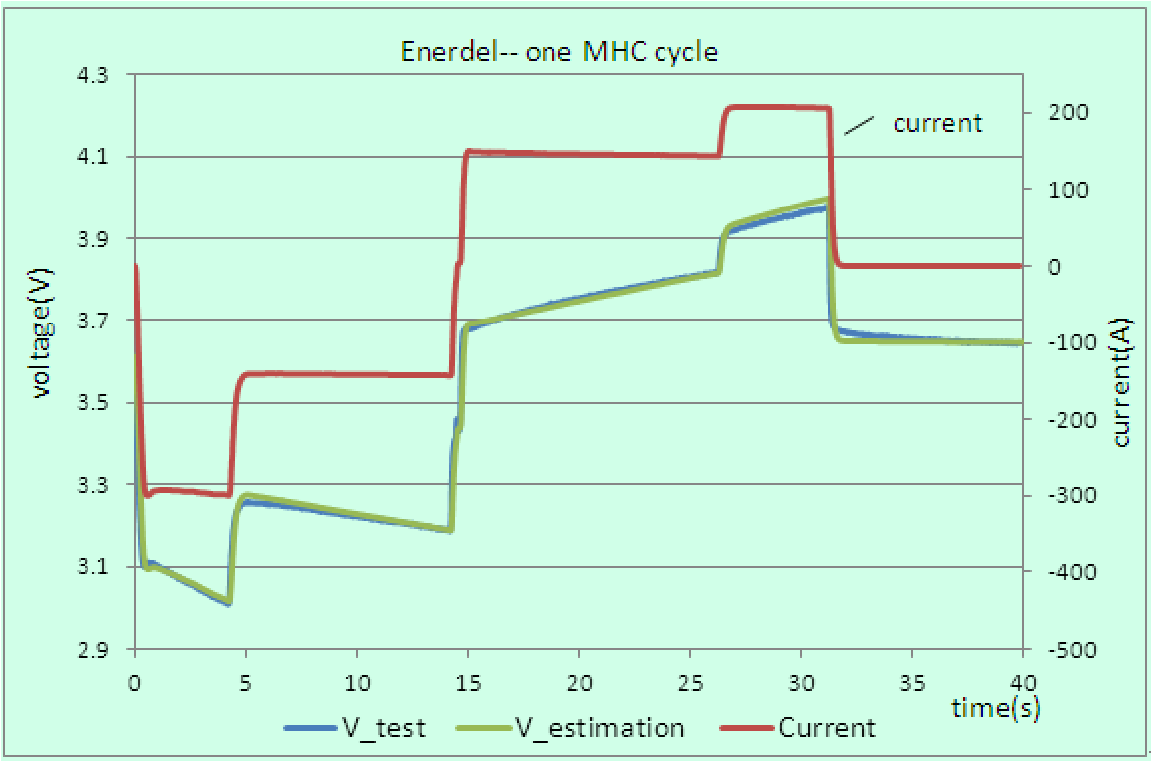

Figure 27 Enerdel MHC Simulation

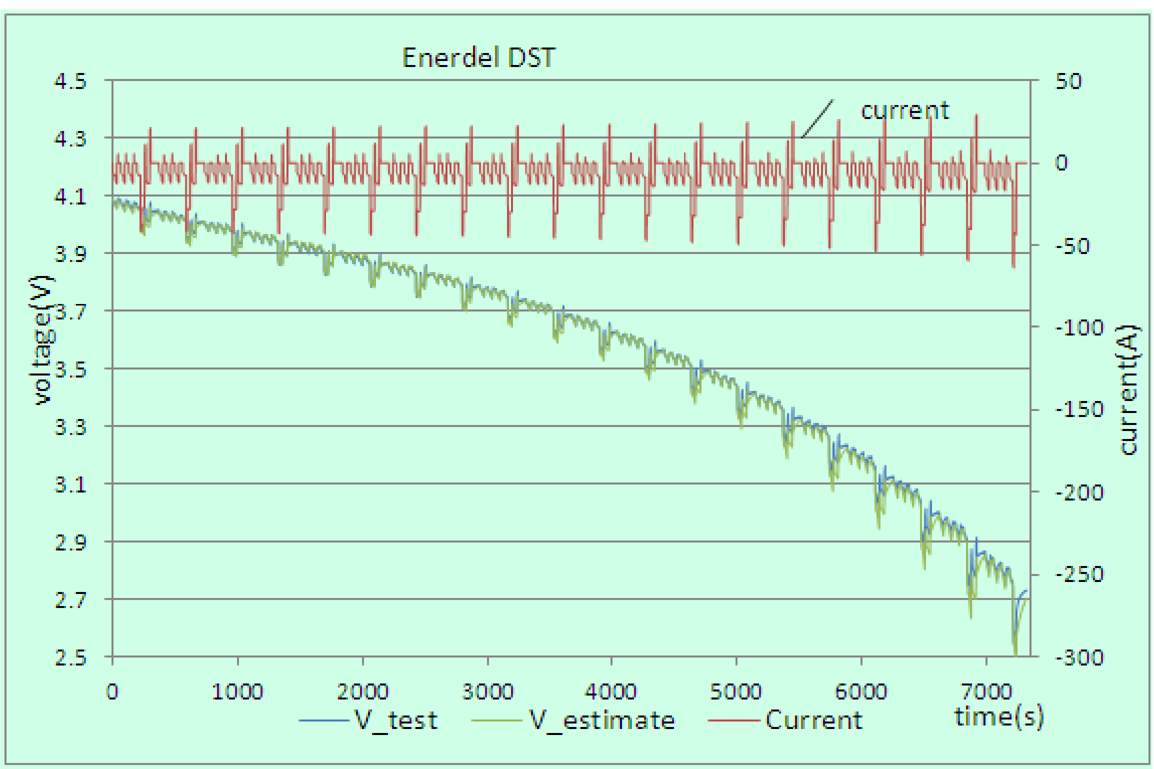

Figure 28 Enerdel DST simulation

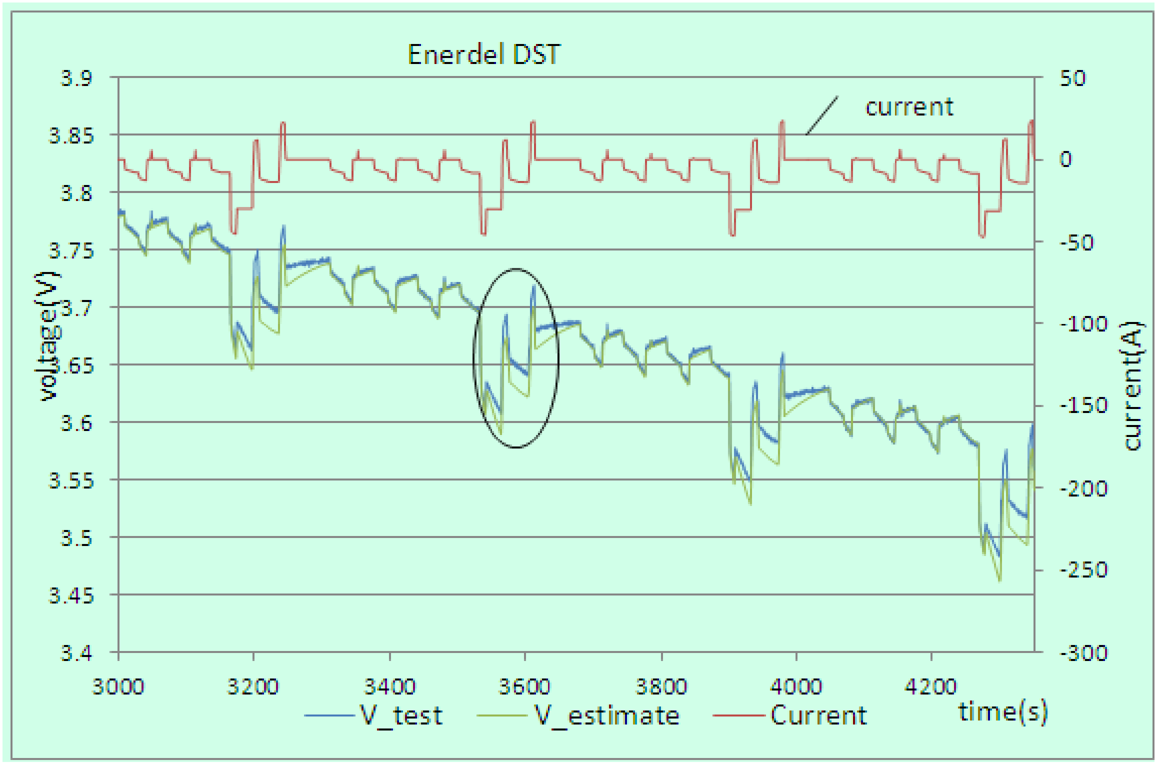

Figure 29 Four of the DST Cycles of an Enerdel Cell

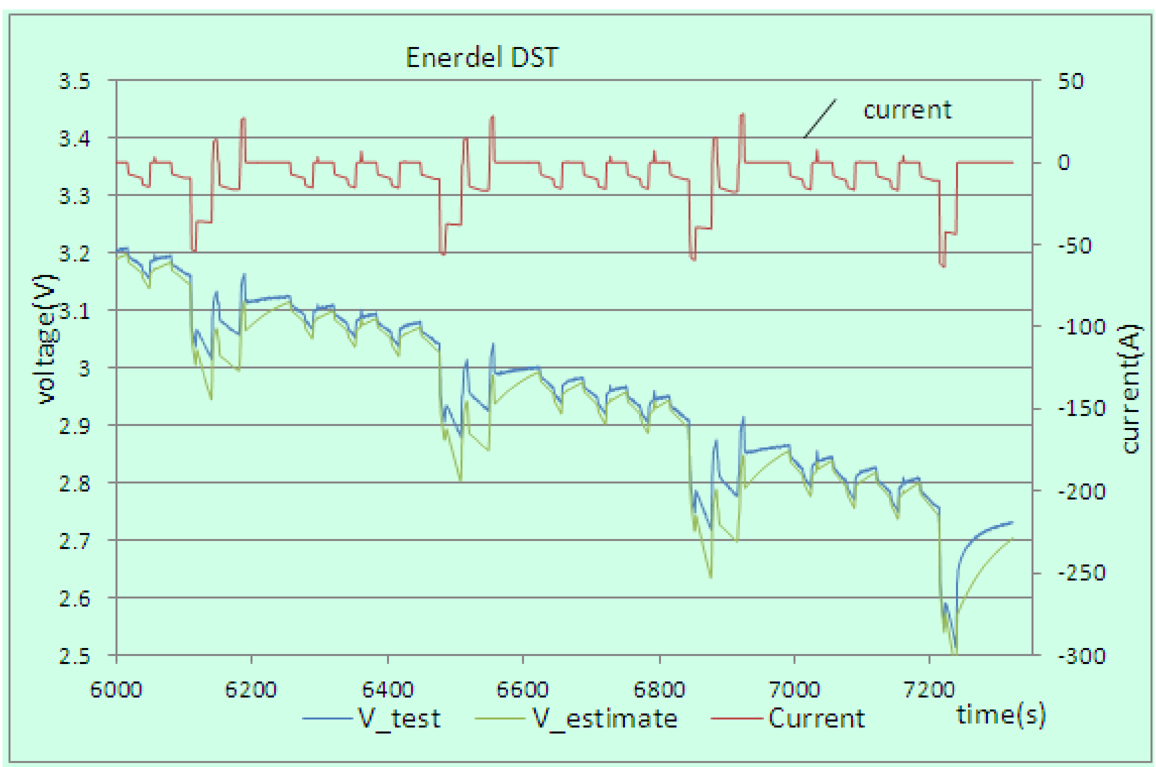

Figure 30 Enerdel last three DST cycles

e. General comments

An open-circuit voltage hysteresis exists for an Enerdel lithium nickel manganese battery (see Figure 26). This hysteresis makes determination of SOC difficult for this chemistry. From Table 11, the “DCH” and “CHR” ohmic resistances are nearly the same and have the same tendency, but the “DCH” values are a little larger than the “CHR” values. The polarized resistance R1 varies with state-of-charge.

In the MHC test, the estimated voltage fits the test voltage well. The first-order transient response model can be applied to simulate a lithium nickel manganese battery dynamically at a fixed SOC. In the DST test, the estimated output voltages only fit the test voltage well when the current is small. The deviation in Figure 29 is mainly due to inaccurate polarization simulation. It seems like that the polarization effect is influenced by current heavily even at a fixed SOC for this battery. For this battery, the polarization effect is more complicated than other cells we have analyzed. .

4.6 Tests for Small Cells

For the small cells (No. 6-8), it is not possible to test them at C/10 to get the Hyst-SOC-OCV curve and on the Dynamic Stress Test cycle, because the currents are too low for the Bitrode. Thus only MHC tests are done on these cells to evaluate the model at a fixed SOC. The circuit parameters of these three small cells at 0.5 SOC are given in Table 12.

The MHC test current and voltages and the estimated output voltage from the model for the Quallion-SA lithium nickel cobalt cell (No. 6), the Quallion-F cell (No. 7) and the K2 lithium iron phosphate cell (No. 8) are shown in Figures 31-33, respectively.

Table 12: circuit parameters of small cells at SOC=0.5

Cells	R0(mΩ)	R1(mΩ)	Tau1(sec)
Quallion SA	63.89	63.06	49
Quallion F	94.68	48.61	51
K2	21.63	16.81	28

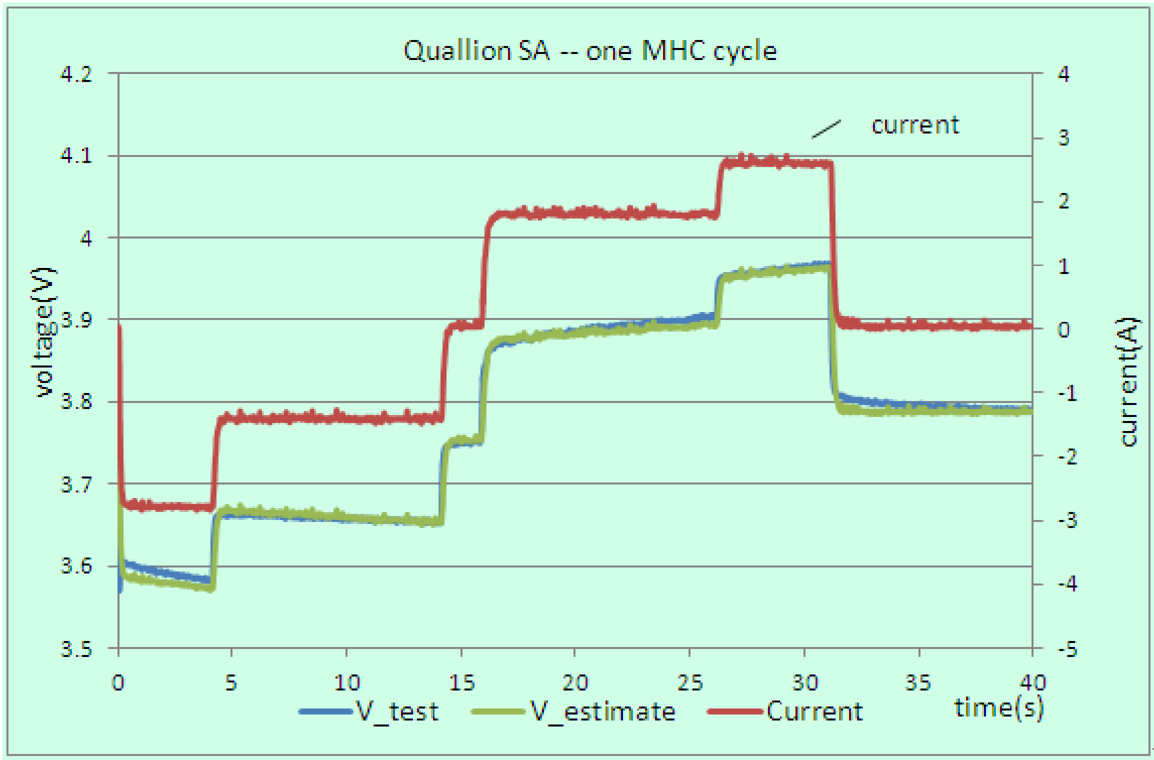

Figure 31 Quallion-SA MHC Simulation

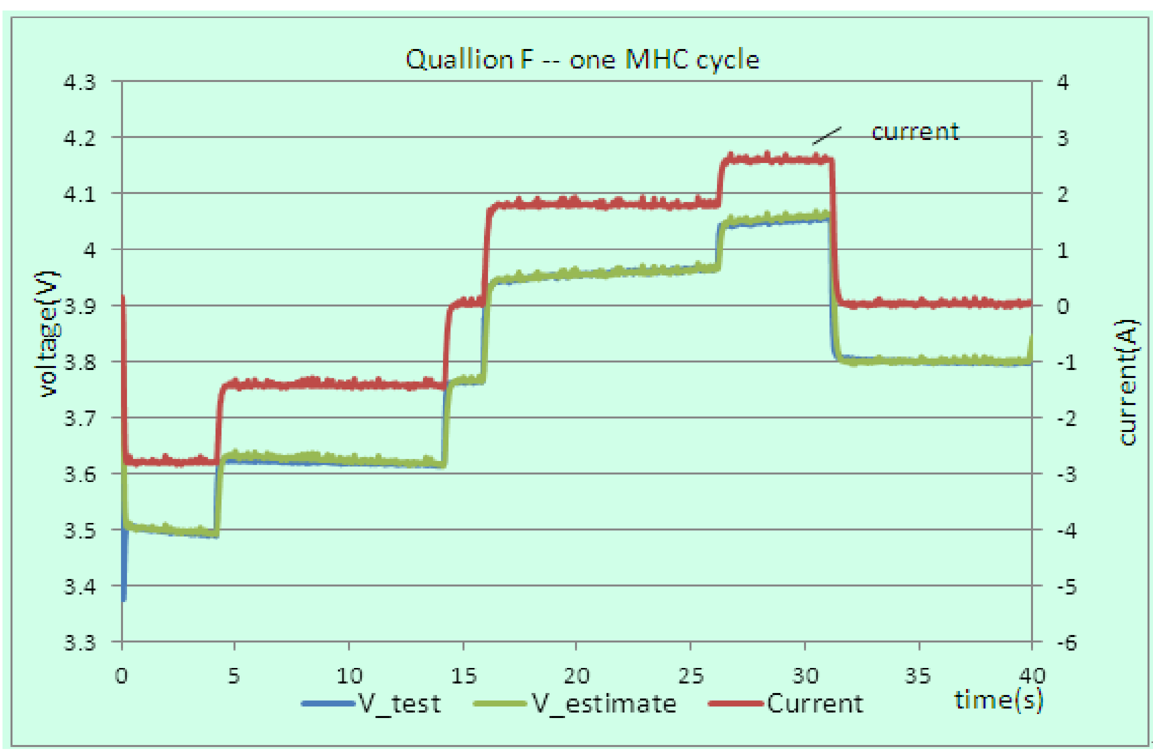

Figure 32 Quallion-F MHC Simulation

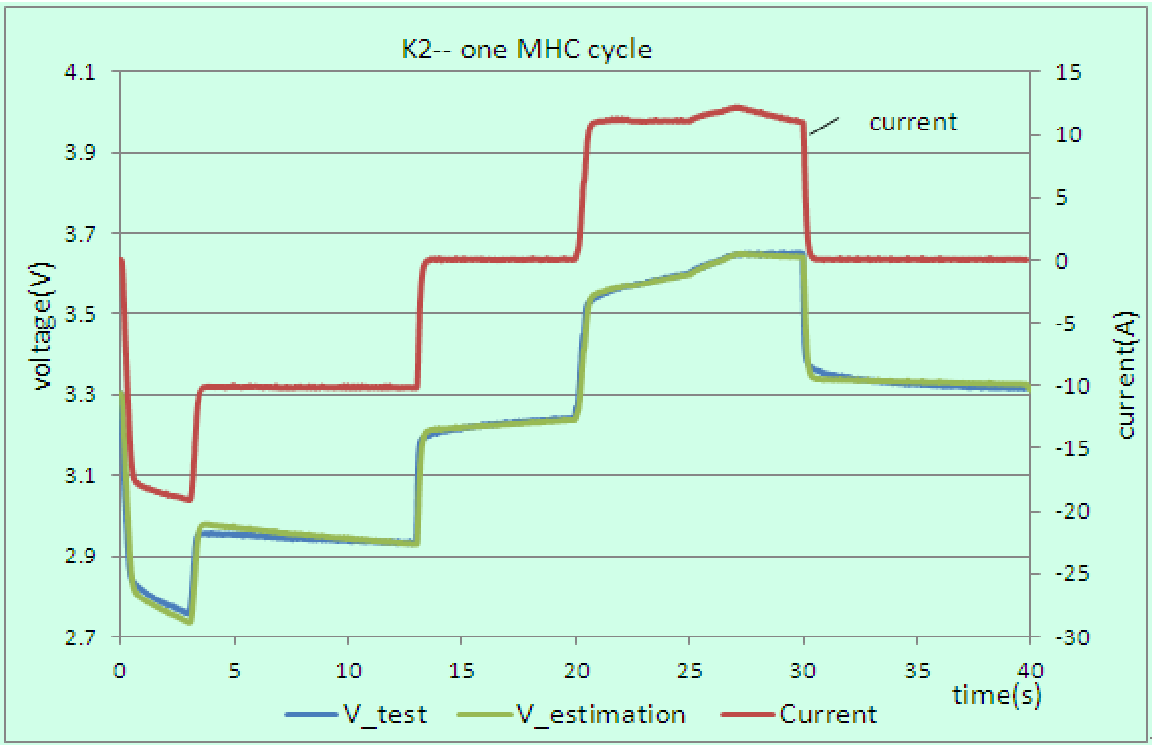

Figure 33: K2 MHC Simulation

For the MHC test cycle, the estimated voltages fit the voltage test data well for all the small cells. Hence, the first-order transient response model can be used to estimate the response of the small cells as well as the larger cells previously studied.

4.7 Other Test Results

a. Dependency of Ah capacity on discharge Rate (nC)

For most batteries, the Ah discharge capacity is dependent to some extent on discharge rate nC. Relevant data for several lithium chemistries [2, 3] are given in Table 13-16. In general, for lithium-ion chemistries there is not a strong dependency of capacity on discharge rate until at least 4-5C and the capacity at 1C is a good measure of the capacity for vehicle applications. The Ah capacity of iron phosphate cells is particularly insensitive to discharge rate.

Table 13: Enerdel HEV high power 15Ah cell (lithium nickel manganese)

Current(A)	nC	Time(sec)	Capacity(Ah)	Ah/(Ah0)
20	1.3	2648	14.7	0.98
40	2.7	1294	14.4	0.96
60	4	844	14.1	0.94
90	6	533	13.8	0.92
120	8	409	13.6	0.91

Table 14: Kokam 30Ah high power cell (lithium nickel cobalt manganese)

Current(A)	Current Rate	Capacity(Ah)	Ah/(Ah0)
15	0.5C	30.9	1.03
30	1C	30.1	1.00
60	2C	28.8	0.96
100	3.33C	27.1	0.90
150	5C	25.1	0.84

Table 15: A123 cell (lithium iron phosphate):

Current(A)	Current Rate	Capacity(Ah)	Ah/(Ah0)
5	2.5C	2.06	1.03
10	5C	2.05	1.025
20	10C	2.09	1.045
30	15C	2.06	1.03

Table 16: K2 2.5Ah cell (lithium iron phosphate)

Current(A)	Current Rate	Capacity(Ah)	Ah/(Ah0)
2.5	1C	2.35	0.94
5	2C	2.43	0.972
10	4C	2.44	0.976
15	6C	2.43	0.972
20	8C	2.42	0.968
25	10C	2.40	0.96
30	12C	2.37	0.948

b. Comparison of CCCV Discharge and CC Discharge

As explained in Section 3.2, the CCCV (constant current, constant voltage) discharge procedure was used in this study to determine the Ah capacity of the cells. The discharge capacities of the various cells in the CV (constant voltage) step at the end of the discharge are shown in Table 17. The percentage of the total capacity that occurs during the CV step depends on the cell chemistry. For the lithium titanate cell, essentially zero occurs in the CV step, but for the lithium iron phosphate cell, the CV step capacity can be as large as 6.9% of the total capacity, which can result in a significant OCV voltage change when the state-of-charge is near 0 or 1. This is the reason why we use CCCV discharge capacity instead of CC discharge capacity.

Table 17: CV Discharge Step Capacity

Cell	CV step capacity (Ah)	Total Capacity (Ah)	Percentage (%)
Altairnano 50Ah	0*	50.8	0
EIG NiCo	0.1	18.3	0.55
EIG LFP	0.7	10.1	6.93
Kokam	1.5	28.2	5.32
Enerdel	0.2	14.3	1.40

* The test data is less than 0.01Ah

c. Scaling of Circuit Elements Based on Ah Capacity

A 100Ah cell can be thought of as a parallel arrangement of ten 10Ah cells of the same technology. The equivalent circuit parameters of the two arrangements would be related as shown below.

$R_{100\,Ah} = 1/10\ R_{10ah}$, $C1_{100Ah} = 10C1_{10Ah}$ and $Tau1_{100Ah} = Tau1_{10Ah}$.

Hence to a reasonable approximation for cells of the same technology and different Ah, the scaling of the circuit parameters for the cells can be expressed as the following:

Resistances: Ah x resistance = constant
Capacitance: capacitance x1/Ah = constant
Tau1 (RC) : Tau = constant independent of Ah

It is of interest to see whether the cells tested seemed to follow the scaling rules given above. The cell circuit scaling parameters for selected cells are shown in Table 18.

Table 18: Scaling of the circuit parameters of different Ah cells of the same chemistry

cells	chemistry	Capacity Ah	R0 mΩ	R0*cap X 10^{-3}	R1 mΩ	R1*cap X 10^{-3}	Tau1 sec
K2	LFP	2.2	21.63	47.59	16.81	37	28
EIG LFP	LFP	10.1	3.92	39.63	2.71	27	21
Quallion-F	NiCo	1.8	94.68	170.43	48.61	87.5	51
Quallion-SA	NiCo	1	63.89	63.89	63.06	63	49
EIG NiCo	NiCo	18.3	4.30	78.67	3.01	55	43

In no case is the scaling exactly as postulated. This is not surprising because in no case are the battery design technologies the same. In fact, the small cells are spiral wound and the big cells are pouch type. Even with these differences, the scaling factors are reasonable except for the resistance of the Quallion-F cell. It is of particular interest to note that the Tau values seem to scale well for the two chemistries. Hence as a first approximation it seems reasonable to use the postulated scaling factors for characterizing batteries of different capacities in vehicle simulations. Otherwise test data would be needed for any cell used in the simulations.

5. Summary

In this report, a first-order transient response battery model is presented. The model can be utilized in the simulation of electric vehicles to calculate the battery voltage for dynamic operation of the vehicle on various driving cycles. The complete battery model requires knowledge of the battery Ah capacity, the hyst-SOC-OCV curve and parameters of the equivalent circuit (R_0, R_1, tau1). The circuit elements are assumed to be a function of state-of-charge, but not of the current.

In order to validate the applicability of this first-order transient response model for various lithium-ion battery chemistries, a number of cells of the different chemistries were tested on charge / discharge step current profiles to determine the circuit parameters for a series of states-of-charge. The cells were then tested on the MHC and DST variable current profiles to determine how well the model predicted the response of the cells to the dynamic profiles. For DST test, the output voltages from the model for all the eight cells tested followed the test voltages well with the errors being relatively small –usually less than 20mV. For MHC test, the tests were performed at a nearly fixed SOC, and the errors were particularly small.

During the DST test, the battery SOC is varied over the complete range (0 to 1). These tests were done for the large pouch cells of the various chemistries. In general, it was found that the model predictions fit the data well in the SOC range of .1-.9, but significant errors occurred near full and empty states-of-charge. This is not surprising because at these states-of-charge the circuit parameters can be changing rapidly. For the 20Ah lithium nickel cobalt cell, the model output voltage fits the test data in 0.1~0.9 SOC range with the error being smaller than 25mV. The circuit elements are stable in this SOC range. For the 11Ah lithium iron phosphate cell, the first-order transient response model voltage fits the test data in 0.23-0.85 SOC range. The error is smaller than 30mV. The circuit elements R0, R1 and Tau1 are stable in the middle SOC range, while polarized resistance R1 is several times larger when SOC is near 1 or 0. For the 30Ah lithium nickel cobalt manganese cell, the model output voltage fits the test data in 0.13-0.94 SOC range. The error is smaller than 30mV. For the 15Ah lithium nickel manganese cell, the model output voltage can follow overall tendency of the test data, but the deviation is significant at high currents. This is mainly caused by the unstable polarization for this cell.

It is interesting to note that the resistances in discharge are in most cases a little larger than the resistances for charging. This seems to mean that it is harder for the lithium ions to insert into the cathode than into the graphite anode. All the cells tested are commercial cells.

In order to prevent lithium plating in the anode, battery manufacturers make the anode to cathode capacity ratio (A/C ratio) larger than unity. That may explain the differences observed in discharge and charge resistances.

The final sections of the report consider the dependency of the discharge Ah capacity on discharge rate (nC) and the final finishing step at constant voltage (CV) and how the circuit parameters can be scaled with cell Ah capacity. It was concluded that for lithium cells, the Ah capacity at 1C is a good measure of cell capacity for vehicle applications. Then CV discharge capacities for the various cells were measured and it was found to be reasonable to add a CV step when discharging a battery. Further it was concluded that the resistances can be scaled reasonably close to inverse with Ah and that tau1 is independent of Ah capacity for a specific cell chemistry and technology.

In brief, the study showed that over most of the useable state-of-charge range, the first-order transient model can be applied to predict the voltage response of lithium-ion batteries to dynamic charge and discharge currents encountered in vehicle applications. This requires knowledge of the cell circuit parameters and OCV as functions of the SOC from prior testing of the cells.

Reference:

[1] PNGV Battery Test Manual, Rev 3, 2001

[2] A. F. Burke, M. I Miller. Performance Characteristics of Lithium-ion Batteries of Various Chemistries for Plug-in Hybrid Vehicles, EVS24 International Battery, Hybrid and Fuel Cell Electric Vehicle Symposium, Norway, 2009

[3] A. F. Burke, M. Miller. The power capability of ultracapacitors and lithium batteries for electric and hybrid vehicle applications, Journal of Power Sources 196 (2011): 514–522

[4] ELECTRIC VEHICLE BATTERY TEST PROCEDURES MANUAL, REV 2, 1996